Sustainable Energy & Fuels

REVIEW

View Article Online
View Journal





Cite this: DOI: 10.1039/c8se00565f

# Supercritical water gasification of biomass: a state-of-the-art review of process parameters, reaction mechanisms and catalysis

Jude A. Okolie,[a] Rachita Rana,[a] Sonil Nanda,[b] Ajay K. Dalai *[a] and Janusz A. Kozinski[c]

The global energy demand has laid emphasis on the exploration of alternate sources of energy. With the application of many thermochemical and biochemical technologies, waste biomass can be converted into green fuels. Gasification is one of the most effective thermochemical (biomass-to-gas) technologies that can transform organic substrates into combustible syngas. Supercritical water gasification is an iteration of conventional gasification that uses water as the reaction medium to efficiently decompose biomass to hydrogen-rich syngas. The yields and composition of products from supercritical water gasification largely depend on the process parameters such as temperature, pressure, residence time, and feed concentration, biomass particle size, reactor configurations as well as reaction pathways and catalysis. These factors also determine the gasification efficiency, carbon conversion and heating value of the gas products. This paper reviews different homogeneous and heterogeneous catalysts involved in supercritical water gasification of biomass. Several reaction mechanisms occurring during gasification of biomass in supercritical water have also been illustrated and discussed, and research gaps for future studies have been identified. Overall, this review is an update to the compiled literature and the aspects involved in supercritical water gasification of different biomass feedstocks.

Received 21st November 2018
Accepted 30th November 2018

DOI: 10.1039/c8se00565f

rsc.li/sustainable-energy

## 1. Introduction

The concerns over the environmental pollution caused by fossil fuels along with their rising prices seem to be alarming. It has become imperative to explore new technologies that can aid in the production of environmentally friendly yet reliable energy

[a]Department of Chemical and Biological Engineering, University of Saskatchewan, Saskatoon, SK, Canada. E-mail: ajay.dalai@usask.ca; Fax: +1-306-966-4777; Tel: +1-306-966-4771

[b]Department of Chemical and Biochemical Engineering, University of Western Ontario, London, ON, Canada

[c]Department of Chemical Engineering, University of Waterloo, Waterloo, ON, Canada

*Mr Jude Okolie is presently a PhD Student and Research Assistant in the Department of Chemical and Biological Engineering at the University of Saskatchewan, Saskatoon Canada. His current research focuses on the supercritical water gasification of lignocellulosic biomass for hydrogen production. Before undertaking his doctoral studies in 2017, Jude worked as a Research Assistant for Michael Okpara University of Agriculture, Nigeria where he was actively involved in research areas relating to the production of sustainable fuels from biomass and biowaste materials and the production of biobased polymers.*

*Ms Rachita Rana is a Research Assistant in the Department of Chemical and Biological Engineering at the University of Saskatchewan, Saskatoon, Canada. Her current research includes the application of supercritical fluid technology for generation of energy from renewable feedstocks and effective remediation of petrochemical waste streams. Her M.Sc. research was focused on the impact of fine particle deposition during hydrotreating of bitumen-derived gas oils. She has keen interest in exploring unconventional fuel generation from oil sands and biomass and synthesis of smart nano-materials.*

resources. Organic waste residues in the form of forest and agricultural biomass, energy crops, microalgae, municipal solid wastes, sewage sludge, cattle manure *etc.* are abundantly available throughout the world and have tremendous potential to be used as feedstocks to produce biofuels.[1] These waste substrates can be converted to fuel products through biochemical technologies (*e.g.* fermentation and anaerobic digestion) and thermochemical technologies (*e.g.* pyrolysis, liquefaction, gasification and torrefaction).[2] Specific green fuels products are obtained from these different technologies. For example, biomass pretreatment and fermentation mostly result in bioethanol and biobutanol using suitable bacterial or fungal species while anaerobic digestion chiefly generates methane by methanogenic bacteria.[3] Bio-oil is the main product of interest from pyrolysis and liquefaction, whereas synthesis gas ($H_2$ and CO) is the chief fuel product from gasification.[2,4]

Biomass is one of the most plentiful renewable resources on the earth and is regarded as a potential raw material to produce sustainable biofuels and value-added chemicals.[5] The fuels produced from waste plant residues are considered carbon-neutral because they do not lead to any greenhouse gas emission and accumulation in the atmosphere. Waste plant biomass not only provides renewable carbon for conversion to biofuels but also fixes $CO_2$ in the atmosphere through photosynthesis. Lignocellulosic biomass provides about 14% of the overall primary energy supply globally, although it supplements about 40–50% of the energy demand in some developing countries.[6] Lignocellulosic biomass, as the name suggests, consists of three primary functional compounds with different chemical structure and weight fractions, namely cellulose (35–55 wt%), hemicellulose (20–40 wt%) and lignin (10–25 wt%).[7] Extractives and ash are also present in smaller quantities in the lignocellulosic biomass. Extractives are the non-structural component of biomass soluble in water or neutral organic solvent (hexane and ethanol). They usually contain biopolymers such as fats, lipids, steroids, terpenoids, wax and phenolic compounds.[7]

Supercritical water gasification (SCWG) is a promising hydrothermal technology for transforming waste biomass to hydrogen-rich syngas at high temperatures and elevated pressures. The supercritical state of water exists at pressures and temperatures above the critical point of water wherein water has no distinct liquid or gaseous phase.[8] Supercritical water (SCW) possesses the dissolution properties of liquids and the diffusion properties of gases. In addition, the high sensitivity of SCW after the critical point towards changes in pressure and temperature makes it an efficient reactant. There is no surface tension during the supercritical state of water as there is no

*Dr Sonil Nanda is a Research Fellow in the Department of Chemical and Biochemical Engineering at the University of Western Ontario, London, Ontario, Canada. His research areas are in the production of advanced biofuels and chemicals from waste and renewable biomass through hydrothermal gasification, pyrolysis, carbonization and fermentation. His parallel interests are in the generation of hydrothermal flames for the treatment of hazardous wastes, agronomic applications of biochar, and phytoremediation of heavy metal contaminated soils, as well as carbon capture and sequestration. Dr Nanda leads many transdisciplinary research projects relating to clean energy, smart materials, sustainable environment and public health.*

*Prof. Ajay K. Dalai is the Professor of Chemical Engineering at the University of Saskatchewan, Canada. He holds the Canada Research Chair position in Bioenergy and Environmental-friendly Chemical Processing. He is a Fellow Member of the Royal Society of Chemistry, the Royal Society of Canada, Chemical Institute of Canada, American Institute of Chemical Engineers, Indian Institute of Chemical Engineers, Canadian Academy of Engineering and Engineering Institute of Canada. His wide-ranging research interests are in Fischer–Tropsch catalysis, bio-oil upgrading, biodiesel production, hydroprocessing of heavy gas oil, dry reforming of methane, gasification and pyrolysis.*

*Prof. Janusz A. Kozinski is the Professor of Chemical Engineering at the University of Waterloo, Canada. Formerly, he was the Founding Dean of the Lassonde School of Engineering in York University, Canada and the Founding President of the New Model in Technology & Engineering in Hereford, UK. He is also a higher education leader, entrepreneur, and an acknowledged expert in sustainable energy systems and immune building concepts applied to public safety and security. His multi-disciplinary research background relates to thermodynamics, space science, and chemical and biological engineering. His notable works are in supercritical water gasification for biofuel production, hydrothermal flames for toxic waste remediation, and next generation nuclear energy reactors.*

liquid and gas phase boundary, as both the phases co-exist.[9] Water beyond its critical pressure of 22.1 MPa and critical temperature 374 °C attains improved mass transfer and solvation properties. Along with high diffusivity like gases and viscosity of a liquid, low dielectric constant is extremely favorable for the use of SCW.[10,11] The viscosity and diffusivity of SCW enhance the reaction rates and enforces particle collision thus contributing in many chemical reactions.

Hydrothermal gasification (or supercritical water gasification) is beneficial over the traditional thermochemical gasification in many ways. When biomass contains high moisture, the process of thermochemical gasification becomes inefficient as the heat of evaporation of the liquid overshadows the heat of combustion of the solid substrate. In such cases, gasification requires drying and pretreatment of biomass adding extra cost to the process economics. However, the large amount of heat required to dry the feedstock makes the entire process inefficient. The rate of reaction is rapid in the case of supercritical water gasification than other gasification treatments.

The major application of SCW is found in the gasification of waste biomass and organics to produce hydrogen.[10–18] The product distribution from SCWG varies largely depending on the process variables such as temperature, pressure, residence time, feed concentration (or biomass-to-water ratio), biomass particle size, reactor configurations and presence of catalyst. Most of the reports on SCWG of biomass currently available in the literature presents scholarly work with inadequate reviews. The current paper aims to review the impacts of these SCWG process parameters on the gas product yields, gasification efficiency, carbon conversion efficiency, hydrogen selectivity and other attributes. Moreover, most of the accessible information on catalysts involved in SCWG of biomass is scattered. This paper compiles the available literature on different homogeneous and heterogeneous catalysts as well as catalyst support applied in SCWG and reviews their reaction mechanisms, performance and activity.

# 2. Supercritical water gasification of lignocellulosic biomass and organic residues

## 2.1. Cellulosic feedstocks

Cellulose is the main structural component of lignocellulose biomass as it typically accounts for 35–55 wt% of lignocellulosic biomass on a dry weight basis. It comprises of D-glucose monomers linked together by β-1,4 glycosidic bonds. The polymer exists in two forms *i.e.* amorphous disorganized structure and the ordered crystalline structure.[19,20] Cellulose has been a preferred model biomass compound for SCWG for two major reasons. Firstly, glucose is the main product of cellulose hydrolysis and a direct monomer. Secondly, glucose is entirely homogeneous, making it easy to study the reaction kinetics and degradation pathway during hydrothermal gasification.

Resende *et al.*[21] reported the non-catalytic hydrothermal gasification of cellulose in a metal-free quartz reactor at 500 °C with 9 wt% feed concentration for 20 min of reaction time. The gas yields obtained were compared with that of another study by Hao *et al.*[22] who used a stainless-steel reactor under the same reaction conditions. The gas yield obtained from the metal-free quartz reactor (8.2 mmol $g^{-1}$) was lower than that from the stainless-steel reactor (18.5 mmol $g^{-1}$). They attributed the increase in gas yield to the reactor wall acting as heterogeneous catalyst, thereby increasing the yield. It is important to note that the contribution of cellulose to $H_2$ production is more than that of hemicellulose and lignin.[23] Therefore, the valorization of real biomass feedstock with high cellulose content for $H_2$ production in SCW is invaluable. Table 1 shows the list of a few biomasses that have been gasified in SCWG.

Sawdust is widely perceived as a waste material from wood processing industries with high cellulose content. Depending on the species, it typically comprises of 47 wt% cellulose, 22 wt% hemicellulose and 20 wt% lignin.[32] In an attempt to study the interactions between each component of biomass, Yoshida *et al.*[32] reported the hydrothermal gasification of sawdust, rice straw and model compounds of cellulose and lignin in SCW at 400 °C and 25 MPa. They observed low carbon gasification efficiency from the real biomass feedstock compared to the model compounds because of the many interactions among each organic and inorganic component present in real biomass. Other biomasses with high cellulosic content that have been explored as some potential feedstocks for SCWG includes wheat straw,[24] fruit shells[26] and rice shell.[37] Demirbas[26] studied the SCWG of five different varieties of fruit shells and suggested that the $H_2$ yield largely depends on the cellulose content of the biomass. The yield of $H_2$ from different fruit shells as reported can be arranged as almond shell > sunflower shell > coconut shell > hazelnut shell > walnut shell.

## 2.2. Hemicellulosic feedstocks

Hemicelluloses is a mixture of $C_5$ and $C_6$ sugars as well as sugar acids including mannose, glucose, xylose, arabinose, galacturonic acid and methylglucuronic acid.[38] Hemicelluloses occur in amorphous form in plants and are the second most abundant component of biomass after cellulose.[20,26] Pure xylan is often used as a model compound of hemicellulose to study the decomposition mechanism and behavior under supercritical conditions as shown in Table 1 although the propensity of its SCWG studies is lesser compared to that of cellulose.

One of the lignocellulosic biomass with high hemicellulose content is water hyacinth. This aquatic weed fits the description of an ideal biomass for hydrothermal gasification because of its high-water content that rather limits its suitability for conventional thermochemical gasification. The plant contains about 25 wt% cellulose, 33 wt% hemicellulose and 10 wt% lignin.[39] Antal Jr *et al.*[34] were the first to study the hydrothermal gasification of water hyacinth and algae in a packed bed reactor at 600 °C and 34.5 MPa. They achieved a complete gasification to generate a gas product with low CO level.

Timothy grass is a perennial grass variety found predominantly in Canadian prairies with high and almost equivalent cellulose and hemicellulose contents (*i.e.* 34 wt% cellulose, 30 wt% hemicellulose and 18 wt% lignin).[7] Nanda *et al.*[33]

Table 1 List of different lignocellulosic feedstocks used in supercritical water gasification

| Biomass | Optimal reaction conditions | Key findings | Reference |
|---|---|---|---|
| Alkaline black liquor from wheat straw | 600 °C, 25 MPa and 12.4 min | • Maximum $H_2$ yield obtained was 11.3 mol $kg^{-1}$<br>• Maximum chemical oxygen demand (COD) removal of 88.7% | Cao *et al.*[24] |
| Cellulose and pinewood | 550 °C, 1 : 7 biomass-to-water ratio and 30 min | • For SCWG of pure cellulose and pinewood, the maximum $H_2$ yield without catalyst was 1.16 and 0.83 mmol $g^{-1}$, respectively<br>• $H_2$ yield increased with the use of KOH catalyst to 9.09 mmol $g^{-1}$ of cellulose and 5.55 mmol $g^{-1}$ of pinewood<br>• Gas yield increased with temperature | Ding *et al.*[25] |
| Cellulose, starch, glucose and cassava | 330–380 °C, 35 MPa and 120 min | • Char yield from starch was lower compared to cellulose<br>• Nearly 0.42 wt% and 0.95 wt% $H_2$ was produced from cellulose and starch, respectively<br>• Glucose had significant $H_2$ yield under subcritical and supercritical conditions | Williams and Onwudili[13] |
| Cellulose, xylan and lignin mixtures | 350 °C and 26–29 MPa | • Presence of lignin affected the gas yield and composition<br>• No interaction between cellulose and xylan was observed<br>• Lignin interacted with other components | Yoshida and Matsumura[23] |
| Fruit shells (almond, cotton, hazelnut, sunflower and walnut) | 476 °C, 48 MPa and 60 min | • $H_2$ yield: walnut shell < hazelnut shell < cotton shell < sunflower shell < almond shell<br>• A correlation was established between temperature and $H_2$ yield, pressure and $H_2$ yield as well as cellulose content and $H_2$ yield | Demirbas[26] |
| Fruit waste and agro-food residues (*Aloe vera* peel, banana peel, coconut shell, lemon peel, orange peel, pineapple peel and sugarcane bagasse) | 600 °C, 45 min, 1 : 10 biomass-to-water ratio and 23–25 MPa | • $H_2$ yield: coconut shell > sugarcane bagasse > *Aloe vera* rind > orange peel > pineapple peel > lemon peel > banana peel<br>• Coconut shell showed high yields of $H_2$ (4.78 mmol $g^{-1}$) and $CH_4$ (3.1 mmol $g^{-1}$) using 2 wt% $K_2CO_3$<br>• Coconut shell had high total gas yields (15 mmol $g^{-1}$) and $H_2$ selectivity (45.8%) due to its high lignin content | Nanda *et al.*[27] |
| Glucose | 750 °C, 28 MPa, 10–50 s and feed flow rate of 240 g $h^{-1}$ | • A simplified model for the reaction pathway for $H_2$ production *via* SCWG was proposed<br>• Maximum $H_2$ yield obtained was 4.78 mol $mol^{-1}$ | Lee *et al.*[28] |
| Kraft lignin | 651 °C, 25 MPa and 3.9 biomass-to-water ratio | • Central Composite Design (CCD) was used to optimize $H_2$ yields<br>• Maximum $H_2$ yield was 1.60 mmol $g^{-1}$ of lignin<br>• Strong interactions between high temperature and water-to-biomass ratio were observed | Kang *et al.*[29] |
| Paper waste sludge | 450 °C, 10 wt% and 60 min | • Ni/$Al_2O_3$–$SiO_2$ catalyst resulted in 5.8 mol $kg^{-1}$ $H_2$ yield<br>• 7.5 mol $kg^{-1}$ of $H_2$ was obtained using $K_2CO_3$ catalyst | Louw *et al.*[30] |

Table 1 (*Contd.*)

| Biomass | Optimal reaction conditions | Key findings | Reference |
|---|---|---|---|
| Pinecone | 550 °C, 23 MPa, 10 wt% and 60 min | • $K_2CO_3$ enhanced water–gas shift reaction while $Ni/Al_2O_3$–$SiO_2$ favored steam reforming and hydrogenation reactions<br>• Supercritical water gasification produced higher gas yield compared to subcritical water gasification<br>• Maximum $H_2$ yield obtained from non-catalytic gasification of pinecone was 1.42 mmol $g^{-1}$<br>• The effectiveness of alkali catalyst to improve $H_2$ yield was in the order of KOH > NaOH > $Na_2CO_3$ | Nanda *et al.*[31] |
| Sawdust, rice straw, cellulose and lignin | 400 °C, 25 MPa and 20 min | • Possible catalyst deactivation by tarry products<br>• Maximum gas and $H_2$ yield from sawdust (6 mmol $g^{-1}$) and rice straw (8 mmol $g^{-1}$) using 0.04 g of Ni catalyst<br>• Different lignin reagents exhibited different gasification behavior | Yoshida *et al.*[32] |
| Timothy grass | 650 °C, 23–25 MPa, 1 : 8 biomass-to-water ratio and 45 min | • Maximum gas yield was 17.2 mol $kg^{-1}$ and $H_2$ yield was 5.15 mol $kg^{-1}$ without catalyst<br>• 3 wt% KOH catalyst increased $H_2$ and total gas yields up to 8.91 and 30.6 mol $g^{-1}$, respectively<br>• Catalyst performance for $H_2$ and total gas yields increased as $Na_2CO_3$ < NaOH < $K_2CO_3$ < KOH | Nanda *et al.*[33] |
| Water hyacinth | 600 °C and 34.5 MPa | • Complete conversion of gas was achieved with little amount of CO produced<br>• No char was obtained after evaporation of liquid effluent | Antal Jr *et al.*[34] |
| Wood sawdust | 300–410 °C, 12–34 MPa and 90 min | • Maximum $CH_4$ yield was 0.33 g $g^{-1}$<br>• Carbon gasification efficiency was dependent on the residence time | Waldner and Vogel[35] |
| Xylose | 600 °C, 21 MPa and 3600 s | • Maximum $H_2$ yield without catalyst was 15 mol $kg^{-1}$<br>• $K_2CO_3$ improved the carbon gasification efficiency (86%) and $H_2$ yield (18 mol $kg^{-1}$)<br>• Product composition was dependent on catalytic activity, temperature and pressure | Gokkaya *et al.*[36] |

proclaimed timothy grass as a dedicated energy crop for SCWG due to its high $H_2$ yields of 5.2 mol $kg^{-1}$ without catalyst and 8.9 mol $kg^{-1}$ in the presence of 3% KOH catalyst. Similarly, the total gas yields increased from 17.2 mol $kg^{-1}$ in non-catalytic SCWG to 30.6 mol $kg^{-1}$ in KOH-catalyzed SCWG. The residues from corn contain 45 wt% cellulose, 35 wt% hemicellulose and 15 wt% lignin.[40] Yanik *et al.*[41] investigated the potential candidacy of corncob as feedstock for $H_2$ production *via* SCWG. The experiments were carried out in a batch autoclave reactor at 500 °C at a heating rate of 3 °C $min^{-1}$ for an hour. Their findings showed $H_2$ yield of 2.09 mol $kg^{-1}$ in SCW. Silver birch is another lignocellulosic biomass containing 40 wt% hemicellulose.[6] Qian *et al.*[6] performed SCW liquefaction of silver birch in an autoclave reactor and obtained about 53.3% bio-oil at 380 °C.

### 2.3. Ligneous feedstocks

Lignin is an essential component of lignocellulosic biomass, which comprises of a branched cross-linked phenyl propane polymer of guaiacyl, syringyl and *p*-hydroxyphenyl units.[42] Many researchers have reported the SCWG of biomass compounds

with high lignin content.[30,35,43] A summary of lignin-rich feedstocks studied for SCWG are presented in Table 1. Coconut shell is a fruit waste with high lignin content as high as 46% with 32% hemicellulose and 14% cellulose.[44] Nanda *et al.*[27] reported the SCWG of coconut shell and other agro-food residues at an optimal temperature of 600 °C with 1 : 10 biomass-to-water (BTW) ratio and 45 min of reaction time. Compared to other agro-food residues studied (*e.g.* banana peel, lemon peel, pineapple peel, orange peel, sugarcane bagasse and *Aloe vera* rind) coconut shell gave a $H_2$ and total gas yields of 2.15 mmol $g^{-1}$ and 7.85 mmol $g^{-1}$, respectively without a catalyst. With 2 wt% $K_2CO_3$ catalyst, coconut shell also produced the highest yields of $H_2$ (4.8 mmol $g^{-1}$) and total gases (15 mmol $g^{-1}$) owing to its high lignification.

In a contrasting study, Yoshida and Matsumura[23] examined the subcritical water gasification of cellulose, xylan and lignin mixtures at 350 °C and 25 MPa to understand the interactions among the three main constituents of lignocellulosic biomass. They showed that there is least interaction between cellulose ($C_6$ sugar) and xylan ($C_5$ sugar), although the contribution of cellulose towards $H_2$ production is more significant than hemicellulose (xylan). Interestingly, the presence of lignin in the mixture inhibited the $H_2$ and gas yields in subcritical water. In subcritical water, the decomposition of lignin proceeds with the initial hydrolysis of its branched primary structures into phenolic compounds (*e.g.* phenol, catechol and guaiacol), aldehydes (formaldehyde) and other low molecular weight compounds.[38] These intermediate compounds undergo cross-linking and re-polymerization to yield high molecular weight compounds such as tars and aromatic chars at moderate temperatures and longer reaction time.[16,45] However, high temperatures during SCWG can lead to hydrothermal liquefaction followed by gasification of lignin, which can also be catalyzed by using alkalis, hydroxides and metals.[33,46] Compared to cellulose and hemicellulose that have low thermal devolatilization temperatures of 250–350 °C and 200–300 °C, respectively, lignin degrades at a much higher temperature range of 200–500 °C.[47]

Waldner and Vogel[35] reported the hydrothermal gasification of woody biomass with high lignin content using RANEY® nickel catalyst. High yields of $CH_4$ (0.33 g $g^{-1}$) were obtained at 90 min with complete gasification using the catalyst. RANEY® nickel also increased the gas yield and eliminated tar formations. In a similar study, Osada *et al.*[43] also reported 30% of gas yield from SCWG of lignin and cellulose at 400 °C using Ru catalyst. The gas phase was enriched with $CH_4$ and the hydrothermal gasification resulted in low char formation. Furusawa *et al.*[48] also performed the SCWG of lignin using 10 wt% Ni/MgO, which demonstrated the best carbon yield (30 wt%) and enhanced carbon gasification efficiency.

Shirai *et al.*[49] evaluated the potential of SCWG as a treatment method to recycle the residues obtained from ethanol production using hard eucalyptus wood. They observed complete gasification of 0.1 g of the residues at 400 °C with Ru/G (graphite-supported 5 wt% ruthenium) catalyst. The gasification results of the ethanol production residue were compared with that of a mixture containing organosolv lignin and cellulose to study the interaction among biomass compounds present in the residue. The observations demonstrated that during the SCWG of ethanol production residue over Ru/G catalyst there is simultaneous gasification of the lignin and cellulose samples present in the residue.

## 3. Degradation mechanism of biomass in supercritical water

For optimizing and enhancing the efficiency of a SCWG process, it is important to understand the decomposition behavior and reaction pathways for each biomass component in SCW. Fig. 1 illustrates the typical reaction pathway of waste degradation during SCWG. Hydrolysis is the first degradation reaction during hydrothermal processing of lignocellulosic biomass. Because of hydrolysis, cellulose breaks down to glucose, hemicelluloses to xylose and glucuronic acid, and lignin to phenolics.

SCWG involves some important sub-reactions to enhance the thermal degradation of biomass into $H_2$. A few of such reactions include water–gas shift reaction, methanation reaction, steam reforming reaction, hydrogenation, dehydration, decarbonylation, decarboxylation and Boudouard reaction. The reactions are illustrated with equations shown below.[50]

Water–gas shift reaction:

$$CO + H_2O \rightarrow CO_2 + H_2 \quad (1)$$

Steam reforming reaction:

$$CH_xO_y + (1 - y)H_2O \rightarrow CO + (1 - y + 0.5x)H_2 \quad (2)$$

Methanation reaction for CO:

$$CO + 3H_2 \rightarrow CH_4 + H_2O \quad (3)$$

Methanation reaction for $CO_2$:

$$CO_2 + 3H_2 \rightarrow CH_4 + H_2O \quad (4)$$

Eqn (5) represents the overall SCW gasification reaction.

$$CH_xO_y + (2 - y)H_2O \rightarrow CO_2 + (2 - y + 0.5x)H_2 \quad (5)$$

The composition of syngas largely depends on $x$ and $y$, where $x$ and $y$ represent the elemental molar ratios H/C and O/C in biomass, respectively.[10,51]

Hydrogenation reaction:

$$CO + 2H_2 \rightarrow CH_4 + 0.5O_2 \quad (6)$$

Boudouard reaction:

$$2CO \rightarrow C + CO_2 \quad (7)$$

$$CO_2 \rightarrow O_2 + C \quad (8)$$

As represented in eqn (1), water–gas shift reaction involves a reaction between CO and water to produce $CO_2$ and $H_2$. The

 

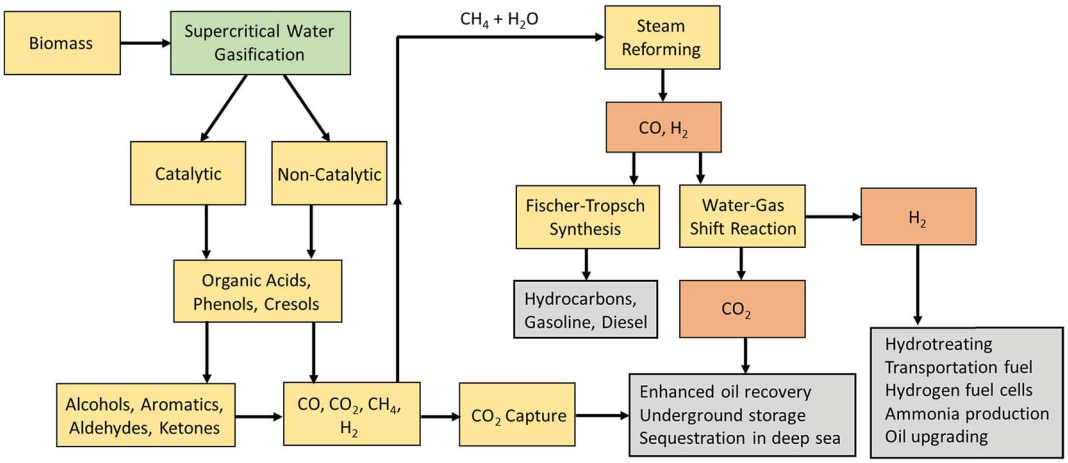


Fig. 1 Reaction pathways involved during supercritical water gasification of biomass.

reaction is favorable at high temperatures and low feed concentrations.[50,52] Steam reforming is also another major reaction that occurs during the SCWG of biomass to produce $H_2$, $CO_2$ and CO (eqn (2)). Hydrogenation and methanation reactions are perceived to be secondary reactions that requires longer residence time and mostly utilizes $H_2$, $CO_2$ and CO to produce $CH_4$ as illustrated in eqn (3), (4) and (6).[17,53] In contrast, Boudouard reaction produces carbon in the form of char or coke from CO and $CO_2$ (eqn (7) and (8)).

Fig. 2 shows the proposed degradation mechanism of cellulose in SCW. For cellulose decomposition, the reaction pathway proceeds with the hydrolysis of cellulose to glucose at temperatures above 200 °C. The initial interaction of subcritical water or low-temperature SCW with cellulose could results in the transformation of its crystalline polymorph to amorphous polymorph through gelatinization.[18] 5-Hydroxymethyl furfural (5-HMF) is formed by the dehydration of glucose. At low temperature (or subcritical conditions), glucose undergoes isomerization to produce fructose and other low molecular weight monosaccharides and disaccharides, erythrose, 1,6-anhydroglucose (levoglucosan) and glycolaldehyde *via* retro-aldol condensation.[54] Erythrose produced during the retro-aldol condensation of glucose provides the basis for which furfurals are formed.[55] In the same way, fructose loses three water molecules *via* dehydration reaction yielding 5-hydroxymethylfurfural (5-HMF) with subsequent polymerization into heavier molecular weight compounds.[56]

5-HMF can form the polyphenol such as 1,2,4-trihydroxybenzene, which is also a key intermediate degradation compound in lignin gasification. Both 5-HMF and polyphenols are degraded to low molecular weight compounds such as aldehydes (*e.g.* acetaldehyde, furfural and formaldehyde),

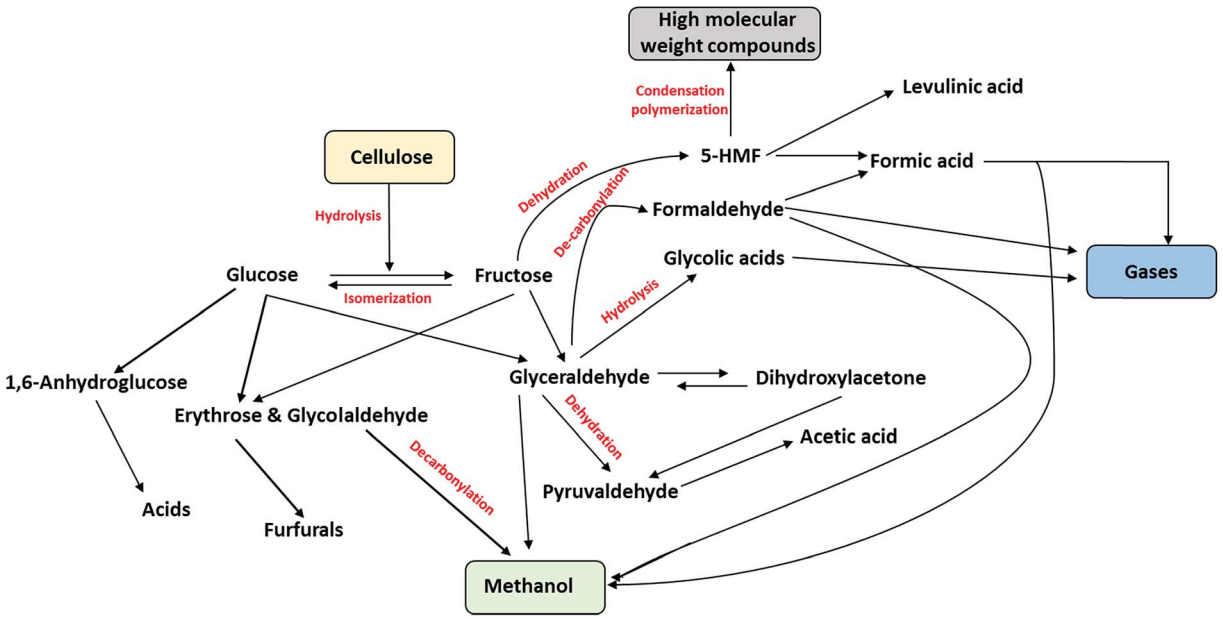


Fig. 2 Proposed degradation mechanism for cellulose during supercritical water gasification.

alcohols (*e.g.* ethanol and methanol), ketones (*e.g.* acetone) and carboxylic acids (*e.g.* acetic acid, formic acid and levulinic acid).[35] The degradation of 5-HMF into levulinic acid and formic acid is also evident at optimal temperatures. Formic acid is further decomposed to form gaseous products rich in $H_2$ and CO. Acetic acid and formic acid are decarboxylated to produce $H_2$, $CO_2$ and $CH_4$. CO can be formed by the either by reverse water–gas shift reaction at high partial pressures of $CO_2$ and $H_2$ or *via* decarbonylation of aldehydes.[35] Fructose also produces glyceraldehyde, which undergoes a series of reactions to produce pyruvaldehyde, acetic acid and dihydroxyacetone products shown in Fig. 2.[55]

The hydrothermal degradation of lignin in SCW is shown in Fig. 3. The decomposition of lignin begins with hydrolysis and dealkylation into formaldehyde and low molecular weight fragments that contain reactive functional groups and compounds such as guaiacols, catechols, syringols and phenols.[56] Because of cross-linking between the low molecular weight compounds and formaldehyde, the residual lignin yields high molecular weight compounds.[57] As shown in Fig. 3, four different phases are obtained because of lignin gasification, namely oil phase, aqueous phase, gas phase and solid residue phase. The ether linkages undergo homogeneous hydrolysis yielding syringols, guaiacols and catechols. The syringols and guaiacols present in the oil phase are transformed into aqueous products such as catechols and methanol in the aqueous phase *via* hydrolysis and dealkylation.[56] The gaseous components such as CO, $CO_2$, $H_2$ and $CH_4$ are evolved at high temperatures through dealkylation when the stable C–C bonds present in lignin and oligomers are cleaved to single-ring and multi-ring phenolics as shown in Fig. 3. Phenolics, aldehydes, methanol, organic acids, hydrocarbons and gases are produced through pyrolysis under hydrothermal conditions.[57]

The decomposition of lignin in subcritical or supercritical water starts with hydrolysis to produce phenols.[43,46] The phenols formed as the intermediate degradation products of lignin from hydrolysis are found to sustain for a longer duration under supercritical conditions.[58] The dehydration of phenolics leads to the formation of aromatic compounds such as benzene, toluene and xylenes, which can pyrolyze and polymerize to form coke.[35] Polyphenols such as dihydroxybenzenes also result from the hydroxylation of phenols. Once again, polymeric compounds such as tars can also result from the condensation of polyphenols. The concentration of phenols formed also influences the decomposition of lignin during SCW gasification and liquefaction.[46,55,57,59] Okuda *et al.*[60] observed the absence of char during SCWG of mixtures containing phenols. The char was suppressed due to the presence of excess phenols. Fang *et al.*[46] showed that the addition of phenols to a mixture containing water and lignin could lead to the degradation of lignin

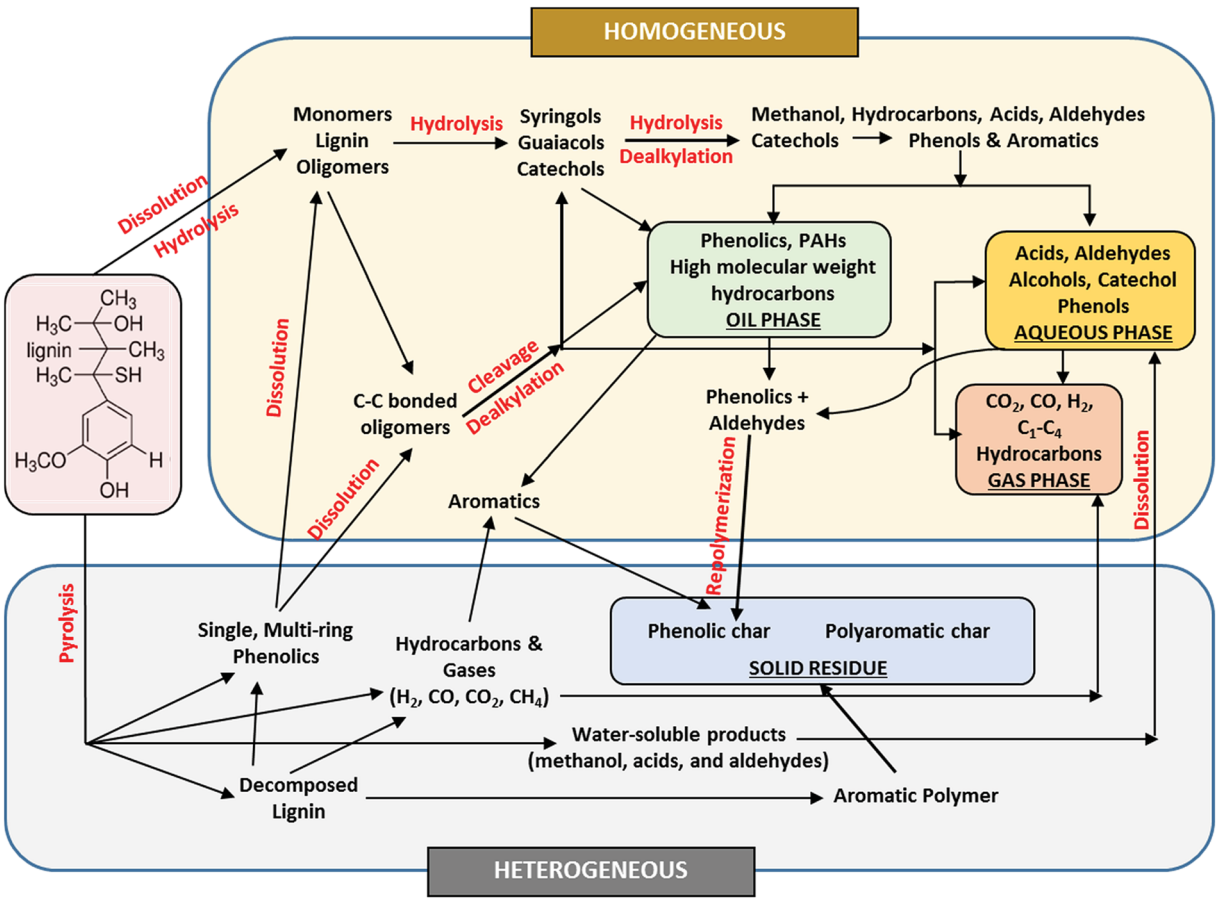


Fig. 3 Proposed degradation mechanism for lignin during supercritical water gasification.

 

thereby preventing further re-polymerization. Alkali salts are known to improve the depolymerization of lignin by either favoring the water–gas shift reaction or suppressing the condensation reactions that proceed after the hydrolysis of lignin. These reactions reduce the char formation and increasing the gas yield. The decomposed lignin might undergo further heterogeneous degradation into condensed chars with cross-linked aromatic compounds.

# 4. Impact of process parameters on SCWG of biomass

## 4.1. Temperature

Temperature is one of the most significant parameters that affects the product yield during SCWG of biomass, especially when the reaction occurs in the absence of catalyst. The operating temperature in SCWG can be grouped into two zones, namely low temperatures (350–500 °C) and high temperature (500–700 °C). There is an increase in CO and $CH_4$ yields in low temperature SCWG, while $H_2$ and $CO_2$ formation is favored at high temperature SCWG.[16] The ionic product mechanism is promoted at low temperature SCWG, whereas the free-radical mechanism is enhanced at high temperature SCWG.[9] The concentration of ionic products of water ($H^+$ and $OH^-$) increase as the SCWG temperature increases, reaching a maximum around 300 °C (subcritical regime) further which they decrease.[61] The splitting of water into ionic products is an endothermic process. Hence, the ionic product mechanism is favored with a rise in temperature. Therefore, subcritical water is a good medium for acid-catalyzed and base-catalyzed reactions. On the contrary, high temperature SCW supplies more hydronium ions ($H_3O^+$) for acid-catalyzed reactions, thereby reducing its pH compared to liquid water. As the pH of SCW medium lowers, the free radical mechanisms are enhanced at high temperatures. The free radical mechanism leads to efficient dissolution of complex organic compounds and their intermediate degradation components to gases.[62] Fig. 4 illustrates the reaction pathways during free radical and ionic mechanisms.

Several researchers have studied the effects of temperature on the gasification yield from both model and real biomass compounds. Many studies have also reported an increment in $H_2$ and $CO_2$ yields as well as carbon gasification efficiency with the increase in SCWG temperature.[31,37,63] Lee *et al.*[28] investigated the gasification of glucose in SCW and studied the effects of temperature on $H_2$ yield. They observed an increase in $H_2$ yield with temperature above 660 °C alongside a decrease in CO yield. The increase in $H_2$ yield at high temperatures is due to water–gas shift reaction and the reduction of CO is due to its consumption as the water–gas shift reactant (CO + $H_2O$). A similar study by Promdej and Matsumura[64] on the SCWG of glucose also supported the findings. The authors grouped the reaction mechanism of glucose degradation into ionic and free radical reactions based on the temperature and kinetic reaction rates. The water–gas shift reaction is a predominant endothermic reaction that involves the reaction of CO with water to produce $CO_2$ and $H_2$ as shown in eqn (1).[51]

As stated earlier, the water–gas shift reaction is completely dominant under high temperature conditions. During SCWG of real biomass (corn starch), D'Jesús *et al.*[65] observed an increase in the gasification product yield with temperature. The gasification yield increased from 0.41 to 0.92 kg of C in the gas per kg of C in corn starch as the temperature amplified from 550 to 700 °C. Demirbas[26] showed that gas yield is mostly dependent on temperature during the gasification of five different fruit shells (*e.g.* almond, cotton cocoon, hazelnut, sunflower and walnut). As the reaction temperature increased from 377 to 477 °C, the gas yield from each fruit shell decreased in the following order: almond shell (6.2–15 wt% of dry basis) > sunflower shell (6.1–11.9 wt% dry basis) > cotton cocoon shell (5.9–12.1 wt% of dry basis) > hazelnut shell (5.1–9.5 wt% of dry basis) > walnut shell (4.9–8.3 wt% of dry basis). In a recent study by Rana *et al.*,[66] SCWG of Athabasca bitumen in a tubular batch reactor showed a rise in $H_2$ yield from 0.42 mmol $g^{-1}$ (at 550 °C) to 0.91 mmol $g^{-1}$ (at 700 °C). At the same time, the amount of CO produced also plummeted. Nanda *et al.*[67] also demonstrated maximum $H_2$ yields (5.16 mol $kg^{-1}$) and total gas yields (10.5 mol $kg^{-1}$) at higher temperature of 675 °C during SCWG of waste cooking oil.

Reaction temperature is a very significant parameter during the hydrothermal gasification of biomass. However, high temperature requirement is also a crucial concern to determine the economics of the SCWG process. The need for high temperature and pressure during SCWG process requires specialized reactor materials that can withstand these extreme reaction conditions. This in turn increases the overall process cost due to the high-energy consumption and durable material requirement. High temperature could reduce reactor plugging and char formation, which are significant problems in SCWG.[68] High temperature and pressure demands in SCW technologies are challenging issues that requires further attention. A cost-effective SCWG technology relies on the following attributes: (i) recovery of waste heat for cogeneration, (ii) development of stable reactor materials that can withstand high-temperature and high-pressure conditions, and (iii) development of novel homogeneous and heterogeneous catalyst to minimize the temperature requirements of the process.

## 4.2. Pressure

The effects of pressure on SCWG process are not clearly understood. According to Le Chatelier's principle, pressure favors the side with the least sum of molecules. To explain the pressure effects, it is essential to consider other competing chemical reactions involved in SCWG. The steam reforming, methanation and water–gas shift reactions as described earlier are the three main competing reactions in hydrothermal gasification.[51] A rise in the pressure will shift the methanation reaction to the right, thereby enhancing the formation of $CH_4$ with the subsequent consumption of CO, $CO_2$ and $H_2$. A rise in pressure could lead to an increase in the water density, ionic product and dielectric constant of water.[10] As the density of water changes with pressure, ionic and free radical reactions are in direct competition.[69] However, as stated by Bühler *et al.*,[70] the

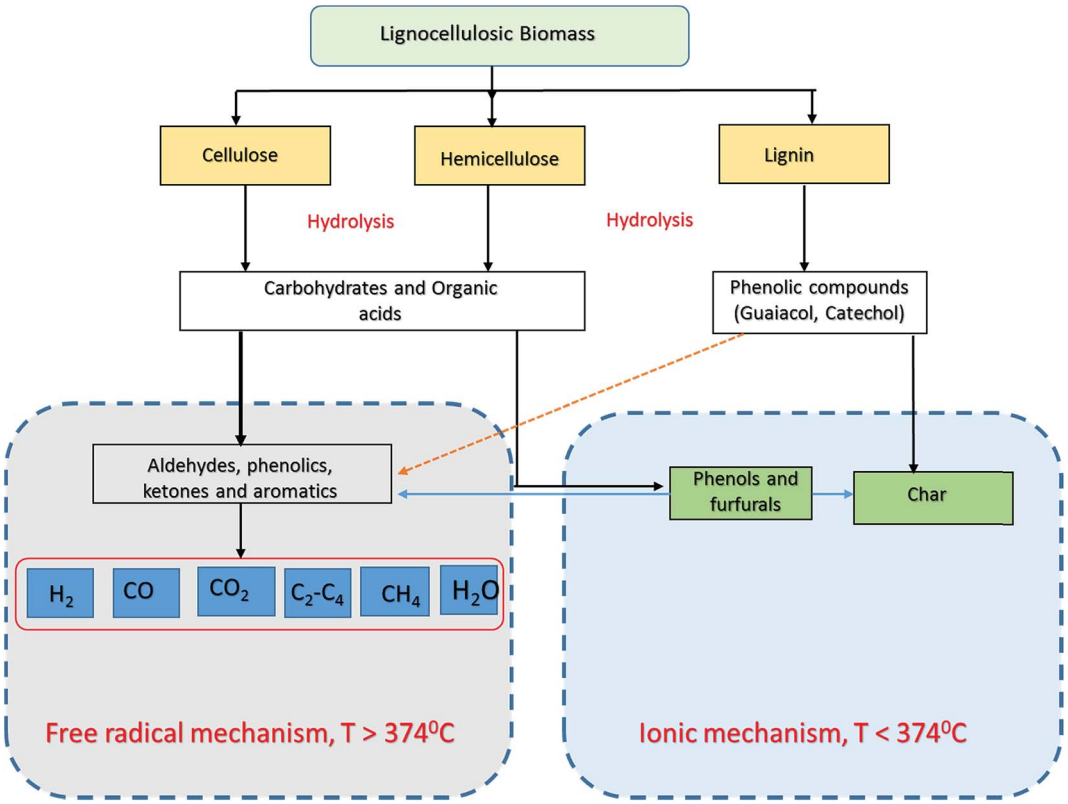


Fig. 4 Ionic and free radical mechanism during hydrothermal gasification of biomass.

ionic reaction is dominant at high pressure due to ionic stabilization at high density of water. Therefore, the rate of ionic reactions increases with pressure while that of free radical reactions decreases.

More specifically, at a constant temperature of 700 °C, the density of water increases with pressure such as: 3.4 MPa (0.008 g $mL^{-1}$) < 6.9 MPa (0.016 g $mL^{-1}$) < 13.8 MPa (0.032 g $mL^{-1}$) < 20.7 MPa (0.049 g $mL^{-1}$) < 27.6 MPa (0.067 g $mL^{-1}$).[71] In the same way, the specific heat, viscosity and thermal conductivity of water also increase with a rise in SCWG pressure. For example, at 700 °C, the viscosity of water at 27.6 MPa (38.6 μPa s) is greater than that at 3.4 MPa (36.7 μPa s). The specific heat of water at 27.6 MPa (50.1 J $mol^{-1}$ $K^{-1}$) is also higher than that at 3.4 MPa (47.9 J $mol^{-1}$ $K^{-1}$). Lastly, the thermal conductivity of water at 27.6 bar (0.118 W $m^{-1}$ $K^{-1}$) is also greater when compared to that at 3.4 MPa (0.095 W $m^{-1}$ $K^{-1}$).

Gadhe and Gupta[71] investigated the gasification of methanol to produce $H_2$ in SCW. Their experimental and equilibrium calculations showed that an increase in the pressure favors methanation reaction, which culminates into a subsequent decrease in $H_2$ yield. From the equilibrium calculations, the $H_2$ yield decreases from 2.75 to 1.5 mol $mol^{-1}$ with an increase in pressure from 3.4 to 25.6 MPa. Similarly, there was also a decline in CO and $CO_2$ yields from 0.9 to 0.3 mol $mol^{-1}$ and 1.0 to 0.6 mol $mol^{-1}$, respectively. As expected, $CH_4$ yield increased from 0.03 to 0.24 mol $mol^{-1}$ under the condition of pressure increase from 3.4 to 25.6 MPa. Therefore, there is an overdependence of individual gas yield on pressure.

Demirbas[26] reported a significant increase in $H_2$ yield with pressure during the SCWG of fruit waste shells. The $H_2$ yield percent rose from 5.9 to 12.6% as the pressure heightened from 23 to 48 MPa. On the contrary, Lu *et al.*[37] observed a slight increase in $H_2$ yield from 15 to 17 mol $kg^{-1}$ when with a rise in pressure from 17.5 to 30 MPa because of the preference of water–gas shift reaction at higher pressures. Similarly, Byrd *et al.*[72] noted a negligible effect of pressure on $H_2$ yield. In their study, 10 wt% of ethanol was gasified in SCW at 700–800 °C with 1.92 g of $Ru/Al_2O_3$ catalyst and a residence time of 2 s. Though the $H_2$ yield increased linearly with temperature, the same was not noticed with pressure. $H_2$ yield increased from 2.6 to 4.5 mol $mol^{-1}$ of ethanol as the reaction temperature elevated from 700 to 800 °C. On the contrary, $H_2$ yield almost remain unchanged (2.6 to 2.7 mol $mol^{-1}$ of ethanol) as the pressure increased from 22.1 to 27.6 MPa.

Kang *et al.*[29] performed non-catalytic SCWG of lignin in a batch reactor with specific focus on understanding the main effects and interaction of temperature (399–651 °C), pressure (23–29 MPa) and water-to-biomass ratio (3–8) on optimization of $H_2$ yields through experimental studies and statistical modeling. The results indicated that high $H_2$ yield of 1.6 mmol $g^{-1}$ biomass was desirable at high temperature of 651 °C. However, increase of pressure from 23 to 29 MPa did not have any significant effect on $H_2$ yield. High temperature had strong interactions with water-to-biomass ratio, but the pressure range studied did not play a key role in any interactions at SCW conditions.

 

### 4.3. Feed concentration or biomass-to-water ratio

To explain the impact of feed concentration on gas yield during SCWG, it is important to consider the involvement of water–gas shift reaction and methanation. Through the water–gas shift reaction, an increase in water will shift the reaction equilibrium to the right, thereby favoring the formation of $H_2$ and $CO_2$. Since the feedstock in SCWG reactor comprises of biomass and water, the feedstock concentration is also referred as the biomass-to-water or water-to-biomass ratio.

When the biomass-to-water ratio is high, it means the amount of water is low compared to the quantity of biomass. Therefore, $H_2$ and CO yield would decrease. At low feed concentration or low biomass-to-water ratio, there is usually an increase in the yields of $H_2$ and $CO_2$ because of higher biomass-to-gas conversion efficiency caused by the higher amount of water than the feedstock.[31] High concentration of water than the biomass quantity results in its improved solvation properties in SCW. In a SCW system, the interactions between high temperatures and low feed concentrations are characterized by a reduction in water density, dielectric constant and ionic product formation as well as an elevation in the solubility potential and free radical formation.[61] At low feed concentration, the low density of water together with less moles of biomass lead to the superior thermal cracking of the organic compounds into gases.

Yu *et al.*[73] varied the concentration of glucose from 0.1 to 0.8 M during SCWG using two different types of reactor materials (*i.e.* Hastelloy C-276 and Inconel 625). In both reactor materials, they observed a drop in the yields of $H_2$ and $CO_2$ by a factor of two as the glucose concentration increased. Lu *et al.*[37] gasified sawdust, rice straw, rice shell and corn cob in SCW and confirmed the findings that at greater biomass concentration, the yields of $H_2$ and $CO_2$ are suppressed. In another study, Nanda *et al.*[53] varied the concentration of fructose from 4 to 10 wt% during SCWG using a continuous flow tubular reactor at an optimal temperature of 700 °C and pressure of 25 MPa and residence time of 60 s. The total gas yield and carbon gasification efficiency decreased from 1.04 to 0.83 L $g^{-1}$ and 88 to 76%, respectively with an increase in feed concentration from 4 to 10 wt%. The $H_2$ and $CO_2$ yields decreased from 3.37 to 2.52 mol $mol^{-1}$ and 3.25 to 1.95 mol $mol^{-1}$, respectively with an increase in fructose concentration. They suggested that a reduced activity of water–gas shift reaction at high feedstock concentration is the main reason for the drop in $H_2$ and $CO_2$ yield. The impaired water–gas shift reaction at high feed concentration results in maximum amount of CO remaining unreacted. However, methanation reaction is promoted at high feed concentration leading to higher concentration of $CH_4$.[17] Although not significant, the yields of $C_2H_6$ is also found to increase with feed concentration.[53]

### 4.4. Reaction time

Reaction time also known as residence time refers to the duration for which the reactants stay inside the reactor. At longer residence times and high temperatures, the gas yields are usually high from SCWG through enhanced thermal cracking reactions.[74] With longer residence times, usually the concentration of CO is reduced because it is consumed as a reactant for many reactions such as water–gas shift reaction, methanation and hydrogenation. Consequently, the concentrations of $H_2$ and $CO_2$ are higher in the gas phase as they are the main products of water–gas shift reaction, whereas $CH_4$ yields are also higher from methanation and hydrogenation reactions.[16,17]

Many researchers have studied the temporal effect on the gas yield from SCWG of biomass and organic waste matter. Guo *et al.*[75] noticed an increase in $H_2$ yield during the SCWG of glycerol from 0.35 to 1.35 mol $mol^{-1}$ as well as a rise in gasification efficiency from 8 to 42% as the residence time was prolonged from 5.2 to 9 s. Similarly, Lu *et al.*[37] observed an increase in the yields of $H_2$ (from 14.5 to 17.5 mol $kg^{-1}$), $CO_2$ (from 16 to 20 mol $kg^{-1}$) and $CH_4$ (from 4 to 8 mol $kg^{-1}$) during SCWG of wood sawdust as the residence time increased from 9 to 46 s. Williams and Onwudili[76] also reported a slight increase in the $H_2$ yield when the residence time was prolonged during the gasification of glucose in SCW. $H_2$ yield increased from 1.26 wt% at 30 min to 1.27 wt% with an increase in the residence time up to 120 min.

The influence of residence time on individual gas yields is also dependent on the effects of other process parameters such as pressure, temperature, feed concentration and reactor type *i.e.* batch or continuous. Lee *et al.*[28] varied the residence time from 10–50 s in a SCWG experiment of 0.6 M glucose between 480 and 750 °C under 28 MPa. They defined residence time as the volume of the reactor divided by the volumetric flow rate of water at a specified temperature and pressure. Their results further elucidate the dependence of residence time on the reaction temperature. At 700 °C, the $H_2$ yield remained almost constant after the residence time exceeded 14 s. They concluded that the $H_2$ yields beyond a particular residence time are not significantly affected. Hence, an increase in residence time could enhance the gas yields up to an optimum point beyond which a subsequent increase would have an insignificant effect on $H_2$ production.[37,65]

Residence time is also dependent on the type of biomass. For instance, for maximum conversion, long-chain hydrocarbons are expected to spend longer time in the reactor compared to short-chain or oxygenated hydrocarbons.[69] Susanti *et al.*[52] studied the effect of residence time on the SCWG of isooctane at a constant temperature of 632 °C, pressure of 25 MPa and 15.25 wt% feed (isooctane) concentration. As the residence time was extended from 6 to 33.3 s, the gas yield increased from 1.1 to 2.9 L $g^{-1}$. Since isooctane is a long-chain hydrocarbon, its complete conversion required a longer residence time.

### 4.5. Biomass particle size

A few studies have investigated the effects of biomass particle size on the gas yield *via* hydrothermal gasification. The low mass transfer resistance of SCW could also negate the impacts of biomass particle size, although the latter affects both heat and mass transfer. Moreover, it cannot be denied that smaller particle size biomass provides higher surface area for higher

degradation and solubility by SCW. To explain the influence of particle size on gas yield during SCWG, it is important to consider the effect of surface area per unit mass of biomass feedstock. Biomass with smaller particles size exhibits larger surface area per unit mass, which makes them exposed to the reaction environment and enhance the heat and mass transfer between the particles. This could increase the efficiency of the gasification reactions and improve the hydrothermal decomposition and subsequent gas yields. However, to obtain the optimal particle size, the cost of energy utilization during biomass size reduction should also be considered.

There are not many studies that report the effect of biomass particle size on hydrothermal gasification of biomass. However, ample amount of information is available in the literature on the effects of biomass particle size on pyrolysis, liquefaction, torrefaction and thermochemical gasification. Therefore, it is important to understand the biomass behavior with different particle sizes in SCWG to optimize the process conditions and maximize gasification efficiency. Lu *et al.*[37] compared hydrothermal gasification results at 650 °C, 25 MPa with 2 wt% rice straw and sodium carboxymethylcellulose for 30 s and varying biomass particle sizes of 40–80 mesh. Biomass with smaller particle sizes *i.e.* <80 mesh size produced higher $H_2$ yield of 17 mol $kg^{-1}$ compared to larger biomass particle size of 40–80 mesh that produced $H_2$ yield of 13.7 mol $kg^{-1}$.

### 4.6. Reactor configurations

Despite the tremendous progress in SCWG research, there is still no large scale reactor design for commercial operation. Small laboratory reactor used for experimental studies are mainly batch reactor (*e.g.* autoclave), continuous flow tubular reactors (CFTR) and continuous stirred tank reactors (CSTR). Batch reactors have a simple design but encounter many disadvantages such as non-isothermal operation. Additionally, the challenges in the isolation of different reactions occurring during the cooling down and heating up stages limit their application for experimental studies with short reaction time.[10] It is also difficult to control the pressure of batch reactors since water exhibit a vapor pressure that is significantly higher compared to that of the produced gas at the reaction conditions. The pressure is dependent on the reaction temperature and the segment of the reactor filled with water.[77]

The schematics of a typical batch reactor are presented in Fig. 5. The use of batch and autoclave reactors for SCWG studies have been demonstrated by many researchers.[25,27,29,31,78–82] A batch reactor classically consists of a nitrogen cylinder, tubular reactor (usually stainless steel or Inconel), high-temperature furnace, temperature control system, thermocouples, pressure gauges, check valves, pressure relief valve, micro-filters, gas liquid separator, desiccant column and gas collection system (either connected to an online gas chromatography system or to gas collection bags). Nitrogen gas is used to create an initial pressure inside the tubular batch reactor, which increases further with the rise in temperature.

Batch reactors are often used for parametric studies to investigate the effect of different operating conditions on the gas yield. Diamond anvil cell (DAC) is a miniature type of batch reactor useful in visualization studies for decomposition behavior of reactants and catalysts during SCWG process.[83,84] DAC is a small volume, high-pressure system that has been applied to investigate the conversion of biomass in a hydrothermal environment as well as temperature-dependent decomposition behavior and solubility of organics.[85] Fang *et al.*[46] used the DAC to study the decomposition behavior of lignin in water/phenol solutions. Similarly, Sasaki *et al.*[86] studied the homogeneous and heterogeneous dissolution and hydrolysis of cellulose in subcritical and supercritical water using a DAC. Reddy *et al.*[16] have made a comprehensive review of hydrothermal gasification of model organic compounds and real biomass using DAC at variable temperatures, pressures, biomass-to-water ratio and other process parameters.

Continuous flow tubular reactors (CFTR) have been utilized in SCWG experiments by a few researchers to carry out continuous experiment over a short residence time that are usually in seconds.[51,53,63,87] Schematic representation of a continuous tubular SCWG reactor is presented in Fig. 6. A CFTR characteristically comprises of a tubular reactor, pre-heater, high-temperature furnace, cooler or condensers, high-pressure prep pump, temperature control system, thermocouples, pressure gauges, ball valves, check valves, pressure relief valve, micro-filters, gas liquid separator, mass flow meter, desiccant column and gas collection system. A high-pressure liquid chromatography pump is used to create pressure and regulate the flow rate and residence time of the feed slurry inside the CFTR reactor.

Despite the promising results obtained using continuous reactor, plugging and non-uniform mixing of the water, biomass and catalysts are some major concerns. Char formations are visible in the heating section of the reactor leading to plugging problems, whereas tar deposits are common in the cooler regions of the reactor.[17,51] It is possible to overcome the plugging issues by applying high gasification temperatures, high heating rate, catalysts and innovative and efficient reaction designs.[37] One of such innovative reaction designs is continuous stirred tank reactors (CSTR) that combines the principles of both autoclave batch reactors and continuous flow reactors.[10] CSTR have uniform mixing and heat distribution with abridged heat and mass transfer limitations. However, CSTR technology still faces major issues such as design complications and high energy requirement for stirring, which requires further development.[88] The fluidized bed reactor is also an alternative to solve the challenges of reactor plugging and char deposition, notwithstanding their complexity for an efficient design.[89,90]

The use of fluidized bed reactors for SCWG of biomass was supposedly proposed by Matsumura and Minowa.[89] The concept was used to achieve a continuous solid handling together with homogeneous reaction atmosphere. Schematic representation of the fluidized bed reactor used in SCWG is shown in Fig. 7. The setup consists of a preheater, cooler, feed loading system, fluidized bed reactor, heat exchangers, pressure regulator, gas–liquid separators, thermocouples and condenser. The fluidized bed reactor consists of an electrical heater coils wound around the outer surface. The heaters are used to heat

 

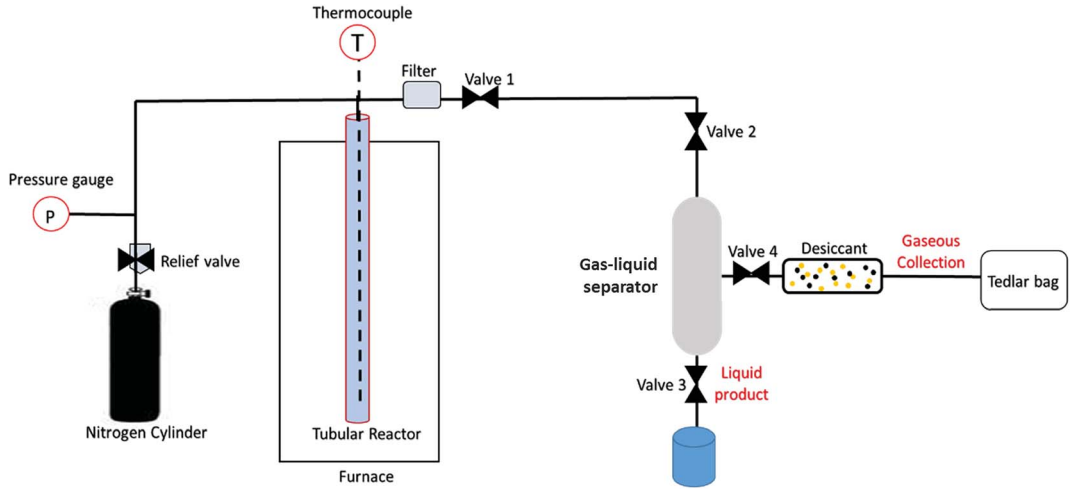


Fig. 5 Schematics of a typical batch reactor used for hydrothermal gasification.

up the reactor to the desired temperature while the thermocouples measure the temperature inside the reactor. Lu *et al.*[91] provided a comprehensive description of the operations of SCWG fluidized bed reactor. Table 2 shows different reactors that have been used to study SCWG process.

Significant progress in SCWG research has led to the establishment of the VERENA pilot plant in Karlsruhe Institute of Technology, Germany[98] and the University of Hiroshima and Chugoku Electric Power Company plant in Japan.[99] The VERENA pilot plant was designed with a throughput of 100 kg $h^{-1}$ of wet biomass with suitability for heterogeneous catalysts. The plant is designed with a maximum allowable pressure and temperature of 35 MPa and 700 °C. One unique feature of the VERENA plant is the presence of a third output unit located at the lower part of the reactor. This unit helps to separate brines and solids, thereby enhancing the ability to handle clogging and minimize fouling of the heat exchangers. Boukis *et al.*[98] reported the SCWG of wet biomass (slurry from corn silage and ethanol) using the VERENA plant.

Compared to the VERENA plant, the University of Hiroshima plant has a throughput of 50 kg $h^{-1}$ of wet biomass and is designed to operate with activated carbon catalyst that is moved with liquid flow throughout the entire plant.[99] Recently, the TU Delft/Gensos semi-pilot scale plant was also established in the Netherlands.[100] The TU Delft/Gensos plant was designed with a capacity of 50 kg $h^{-1}$ wet biomass capacity. The plant uses a fluidized bed reactor with the intent of overcoming the challenges of reactor plugging due to salt deposition and char formation and enhancing heat and mass transfer. Yakaboylu *et al.*[100] gasified starch in the TU Delft/Gensos plant with

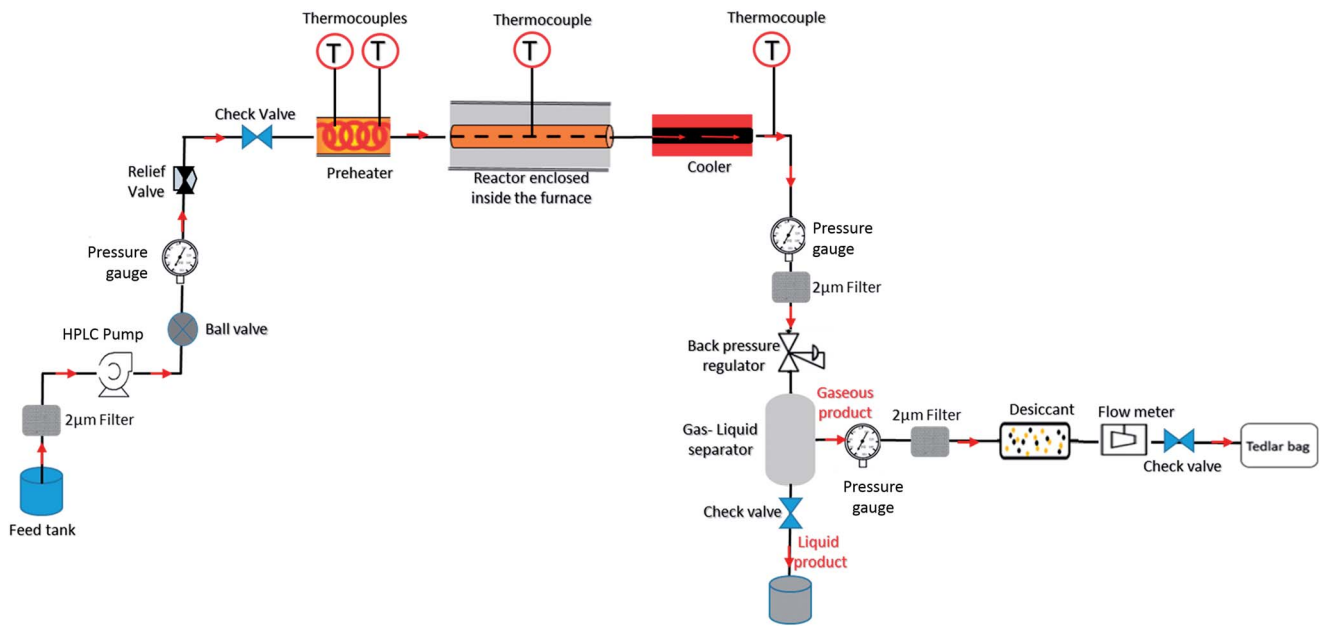


Fig. 6 Schematics of a typical continuous flow tubular reactor (CFTR) used for hydrothermal gasification.

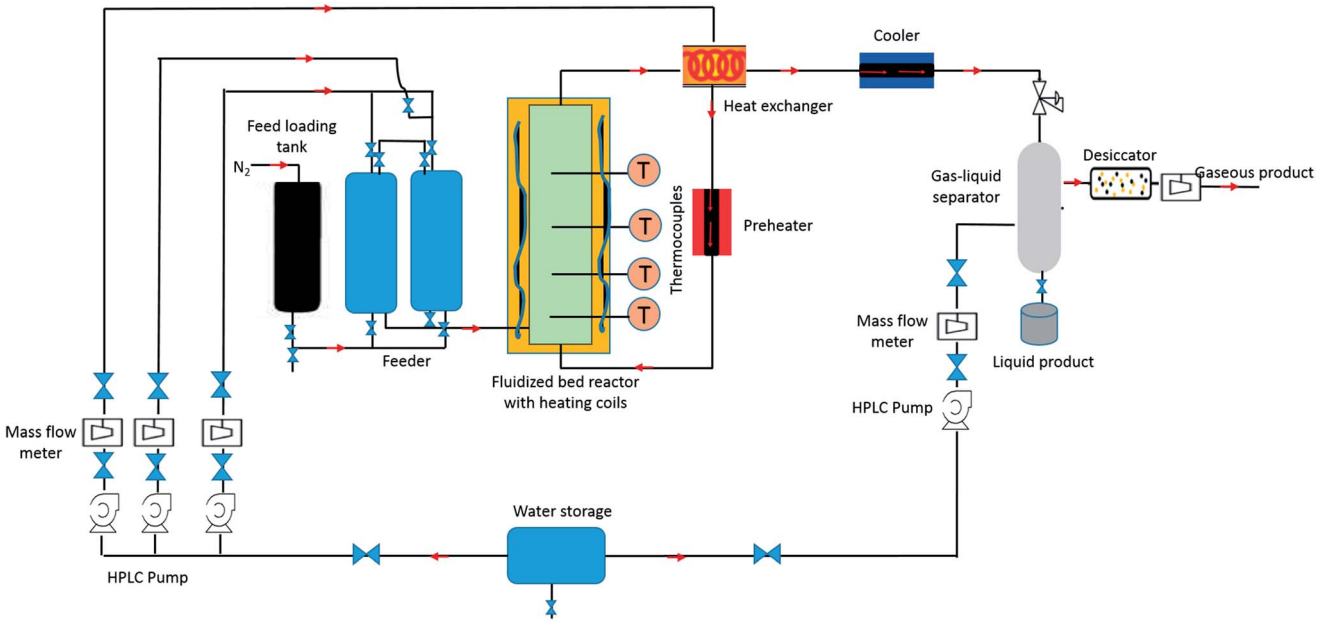


Fig. 7 Schematics of a typical fluidized bed reactor for hydrothermal gasification.

4.4 wt% feedstock concentration at 500–600 °C and tested two flow rates of 4.5 kg $h^{-1}$ and 35 kg $h^{-1}$ at 25 MPa. Their results showed that lower feed rates and high temperatures favor gasification yields. Maximum gasification efficiency of 73.9% was observed at 600 °C and feed flow rate of 24.5 kg $h^{-1}$.

van Wyk *et al.*[101] recently designed and tested a supercritical water desalination pilot plant (SCWD) with maximum throughput of 8 kg $h^{-1}$. The plant which is located at the high-pressure laboratory of the University of Twente is designed to operate at optimal conditions of 500 °C and 38 MPa. To test the performance of the SCWD plant, a base experiment was carried out using a saline feed with 3.5 wt% NaCl after which the stability together with the performance of each unit were analyzed. The experimental findings show that the plant produced higher recovery of drinking water compared to the conventional filtration processes.

## 5. Catalytic supercritical water gasification of biomass

### 5.1. Homogeneous catalysts

SCWG is an energy-intensive process requiring high temperature and pressure, which could possibly lead to high processing cost. Catalysts are used in SCWG to improve the gas yield at the same time minimize the heat requirements. Homogeneous catalysts mostly include the alkali and hydroxide catalysts such as $K_2CO_3$, $Na_2CO_3$, KOH and NaOH. Alkali homogeneous catalysts have an ability to break the C–C bonds and promote the water–gas shift reaction.[9,15,102] Homogeneous catalysts are beneficial because of their low cost, higher and faster conversion rates and flexibility for use in batch and continuous gasification processes.[103] Although homogeneous catalysts are more effective than the heterogeneous catalyst, in some cases they pose serious challenges such as contributing to reactor plugging and corrosion problems.[82] This is because of the low solubility of alkali salt in SCW.[69] Moreover, it is relatively difficult to recycle and reuse homogeneous catalysts after an SCWG experiment. Conversely, heterogeneous catalysts offer a few ways for recovery and reuse with additional expenditures.

Sınağ *et al.*[104] compared the effect of two different catalysts (1 wt% of RANEY® nickel and 0.5 wt% of $K_2CO_3$) on the gas yield and the number of intermediates produced at different heating rates during the gasification of glucose. The authors observed a high catalytic ability of $K_2CO_3$ compared to RANEY®-Ni catalyst. Likewise, the $H_2$ yield obtained with $K_2CO_3$ was twice as much as the yield without a catalyst. They explained the effect of $K_2CO_3$ on $H_2$ yield and $CO_2$ production by using the catalyzed water–gas shift reaction through the formate ($HCOO–K^+$) formation as shown in the eqn (9)–(12):

$$K_2CO_3 + H_2O \rightarrow KHCO_3 + KOH \quad (9)$$

$$KOH + CO \rightarrow HCOOK \quad (10)$$

Formate (HCOOK) reacts with water to produce $H_2$ as follows:

$$HCOOK + H_2O \rightarrow KHCO_3 + H_2 \quad (11)$$

Formation of $CO_2$ and $K_2CO_3$ completes the catalytic cycle.

$$2KHCO_3 \rightarrow CO_2 + K_2CO_3 + H_2O \quad (12)$$

Nanda *et al.*[33] evaluated the SCWG efficiency of timothy grass as an energy crop using four alkali homogeneous catalysts, especially carbonates ($Na_2CO_3$ and $K_2CO_3$) and hydroxide catalysts (NaOH and KOH). SCWG of timothy grass at 650 °C and

 

Table 2 Different types of reactors and catalysts used in supercritical water gasification

| Biomass and model compounds | Optimal reaction conditions | Catalysts | Maximum $H_2$ yield | Reference |
|---|---|---|---|---|
| **Batch reactor** | | | | |
| Cellulose and lignin | 400 °C, 25 MPa and 20 min | Nickel | $H_2$ gasification ratio (1.23 for cellulose and 0.17 for lignin) | Yoshida *et al.*[32] |
| Cellulose, xylan and lignin mixtures | 350 °C, 25 MPa and 20 min | Nickel | 2.52 mmol $g^{-1}$ | Yoshida and Matsumura[23] |
| Fruit waste and agro-food residues | 600 °C, 45 min 23–25 MPa and 1 : 10 biomass-to-water ratio | $K_2CO_3$ and NaOH | 4.8 mmol $g^{-1}$ from coconut shell with 2 wt% $Ka_2CO_3$ catalyst | Nanda *et al.*[27] |
| Humic acid | 600 °C, 75 min and 15 wt% feed concentration | Lewis acid metal chloride catalyst ($AlCl_3$, $CaCl_2$, $CuCl_2$, $FeCl_3$, $NiCl_2$) | 0.79 mol $kg^{-1}$ (non-catalytic) and 11.03 mol $kg^{-1}$ with 15 wt% of $AlCl_3$ | Gong *et al.*[79] |
| Lignin | 651 °C, 25 MPa and water-to-biomass ratio of 3.9 | — | 1.6 mmol $g^{-1}$ | Kang *et al.*[29] |
| Green algae (*Enteromorpha intestinalis*) | 440 °C 25 MPa and 10 min | Ru promoted Ni–Fe/γ-$Al_2O_3$ | 5.25 mmol $g^{-1}$ (non-catalytic) and 12.28 mmol $g^{-1}$ with catalyst | Norouzi *et al.*[92] |
| Sea grass (*Posidonia oceanica*) | 600 °C, 44.2 MPa, 1 h and 0.08 g $mL^{-1}$ biomass loading | — | 10.37 mol $kg^{-1}$ | Deniz *et al.*[93] |
| Timothy grass | 650 °C, 23–25 MPa and 1 : 8 biomass-to-water ratio, 45 min | $Na_2CO_3$, $K_2CO_3$, NaOH and KOH | 5.15 mol $kg^{-1}$ without catalyst and 8.91 mol $kg^{-1}$ with 3 wt% of KOH catalyst | Nanda *et al.*[33] |
| **Diamond anvil cell** | | | | |
| Cellulose and glucose | 360 °C and 30 MPa | Nickel, Pt/γ-$Al_2O_3$ and Ni/silica-$Al_2O_3$ | 44 mol% $H_2$ with glucose using Pt/γ-$Al_2O_3$ catalyst | Fang *et al.*[57] |
| Winery waste | 500 °C, 30 min and 25 MPa | — | Maximum mole fraction of $H_2$ obtained was 33.9% | Bocanegra *et al.*[84] |
| Cellulose | 350 °C, 16.5 MPa and 2.2 °C $s^{-1}$ | Nickel | Maximum gas yield of 74% with 40 wt% Ni | Fang *et al.*[94] |
| **Continuous reactors** | | | | |
| Clover grass and corn silage | 700 °C, 45 MPa and 16.82 min | $KHCO_3$ | 29.7 vol% of $H_2$ was produced from clover grass | D'Jesús *et al.*[65] |
| Fructose | 700 °C, 25 MPa, 60 s and 4 wt% feed concentration | NaOH and KOH | 3.26 mol $mol^{-1}$ of $H_2$ was obtained without a catalyst. $H_2$ yields of 10.67 mol $mol^{-1}$ with 0.8 wt% of KOH and 9.86 mol $mol^{-1}$ with 0.8 wt% of NaOH were obtained | Nanda *et al.*[53] |
| Isooctane | 607 °C, 25 MPa, 8 s and 2300 mmol $L^{-1}$ of $H_2O_2$ | — | 0.63 mol $mol^{-1}$ without $H_2O_2$ and 1.68 mol $mol^{-1}$ with $H_2O_2$ | Veriansyah *et al.*[95] |
| Isooctane | 637 °C, 25 MPa, 18 s and 2701.1 mmol $L^{-1}$ of $H_2O_2$ | — | 2.61 mol $mol^{-1}$ without $H_2O_2$ and 6.13 mol $mol^{-1}$ with $H_2O_2$ | Susanti *et al.*[52] |
| Lactose | 700 °C, 25 MPa, 60 s and 4 wt% feed concentration | $Na_2CO_3$ and $K_2CO_3$ | 16 mol $mol^{-1}$ of $H_2$ was obtained without any catalyst. 22.4 mol $mol^{-1}$ of $H_2$ was obtained with 0.8 wt% $Na_2CO_3$ | Nanda *et al.*[87] |
| **Fluidized bed reactor** | | | | |
| Chicken manure | 600 °C and 24 MPa | Activated carbon (AC) | 25.2 mol $kg^{-1}$ of $H_2$ with 9 wt% AC catalyst | Cao *et al.*[96] |
| Sewage sludge | 540 °C and 25 MPa | KOH, $K_2CO_3$, NaOH and $Na_2CO_3$ | 15.5 mol $kg^{-1}$ of $H_2$ was obtained with 0.5 wt% KOH catalyst | Chen *et al.*[97] |

45 min of reaction time with 1 : 8 biomass-to-water feed ratio gave high yields of $H_2$ (5.15 mol $kg^{-1}$) and total gases (17.2 mol $kg^{-1}$). The application of alkali catalysts significantly improved the $H_2$ yields in the following order: KOH (8.91 mol $kg^{-1}$) > $K_2CO_3$ (7.84 mol $kg^{-1}$) > NaOH (6.68 mol $kg^{-1}$) > $Na_2CO_3$ (6.39 mol $kg^{-1}$) > no catalyst (5.15 mol $kg^{-1}$) .

It is affirmed that alkali catalysts, especially KOH and $K_2CO_3$ helps to catalyze the water–gas shift reaction, thereby producing $H_2$ and $CO_2$ instead of CO. On the other hand, $Na_2CO_3$ causes decarboxylation of formic acid (HCOOH), which is an intermediate product of water–gas shift reaction, thereby increasing the $H_2$ yields.[102,105] Additionally, $Na_2CO_3$ forms precipitated

particles in SCW that subsequently provide larger surface area for many catalytic reactions. In contrast, NaOH promotes $CH_4$ yields by favoring methanation reaction even at subcritical conditions *i.e.* ~350 °C.[33] Hydrolysis of biomass by NaOH produces sodium acetate ($CH_3COONa$) as an intermediate product, which further decomposes to $CH_4$ and sodium bicarbonate ($NaHCO_3$).[106]

Trona ($NaHCO_3 \cdot Na_2CO_3 \cdot 2H_2O$), red mud, borax ($Na_2B_4O_7 \cdot 10H_2O$) and dolomite [$CaMg(CO_3)_2$] are a few other homogeneous catalysts used to improve gas yield during SCWG of lignocellulosic biomass. Yanik *et al.*[41] showed that trona exhibited similar catalytic activity with $K_2CO_3$ during SCWG of lignocellulosic materials. In another study, Madenoğlu *et al.*[107] during the gasification of five selected biomass samples (*e.g.* cauliflower residue, acorn, tomatoes residue, extracted acorn and hazelnut shell) in SCW observed that the $H_2$ yield of acorn increased by seven-folds than without a catalyst. The authors proposed that trona could be used as a substitute to other commercial catalysts. Madenoğlu *et al.*[108] compared the catalytic activity of three different homogeneous catalysts (*e.g.* borax, dolomite and trona) during the hydrothermal gasification of hard-shell nut residues at temperatures of 300–600 °C. The activities were in the following order: trona > borax > dolomite.

### 5.2. Heterogeneous catalysts

Heterogeneous catalysts can be classified into metal oxides and transition metal catalysts. One main advantage of heterogeneous catalysts is the ability to recover and reuse while reducing the cost of catalyst development at the same time adding cost to their recovery. The catalysts are also preferred because of their selectivity and inertness to reside inside the reactor or on the support material. However, deactivation, poisoning and sintering of heterogeneous catalysts due to the presence of sulfur, nitrogen, coke or any other compounds containing heteroatom is still a big challenge. Moreover, the metal cations are transformed into oxides and their corresponding salts during SCWG while elements such as S and Cl are easily oxidized into their corresponding organic acids, which stay in the aqueous phase after the completion of the reaction.[109] The low dielectric constant of water under supercritical conditions means that organic compounds are easily dissolved in SCW while inorganic salts and impurities separates out and are left behind in the reactor.[69]

As mentioned earlier, the transition metal catalyst could be either nickel or other novel metal catalyst. The examples of novel metal catalysts that have been used for SCWG include Pb, Pt, Rh and Ru. Ni-based catalysts are mostly used in SCWG because of its low cost compared to other novel metal catalysts. Although the use of nickel could possibly lead to high total gas yields and improved carbon gasification efficiency, the $H_2$ production is subdued due to the consumption in hydrogenation reaction.[18] Nickel also catalyzes methanation reaction and demonstrating high selectivity towards $CH_4$ in SCWG.[32,45,110,111] However, Resende and Savage[112] reported that $CH_4$ yields are catalyzed by Cu-based catalysts at a significant level compared to Ni and Fe-based catalysts. Low $CH_4$ yields using Ni/$\alpha$-$Al_2O_3$ and Ni/hydrotalcite are also reported from the SCWG of carbohydrates even at high temperatures and longer reaction times.[113]

The main issue with nickel catalyst is the unavoidable problem of sintering and catalyst deactivation by tar-forming products. Li *et al.*[114] reported that the char layer could be avoided by co-precipitation of Ni–Mg–Al catalyst during the SCWG of glucose. They synthesized and tested a series of Ni–Mg–Al catalysts with different molar ratios of Mg/Al. An increase in both $H_2$ yield from 1.7 to 12 mmol $g^{-1}$ and $H_2$ selectivity from 25 to 70% was obtained at a Ni–Mg–Al ratio of 1 : 0.6 : 1.9. Additionally, the presence of Mg could increase the longevity of the catalyst and enhance the anti-carbon formation by the Ni–Al catalyst, thereby hindering graphite formation.

The metal catalysts used in SCWG are either in the supported or unsupported form. A suitable catalyst support could increase the catalytic activity and provide better stability. Supporting material is very important for heterogeneous catalyst due to the strident nature of the SCW environment. The commonly used catalyst support in hydrothermal gasification includes alumina, silica, molybdenum, olivine, metal oxides, activated carbon, carbon nanotubes, graphite, *etc.* Some studies have also reported lignocellulosic biomass as the support material and reactant in hydrothermal gasification studies.[45,109,115–117] In such studies, catalytic metal nanoparticles were impregnated or synthesized in the biomass's cell wall at varying the metal concentrations and doping conditions (*e.g.* temperature, pH, agitation, duration and additives).

Tailoring the catalyst by varying the supporting material is an alternative way to increase the catalytic activity, stability and gas yields. Several studies have reported the use of different types of catalysts support to enhance hydrogen yield during the SCWG of biomass model and real compounds. For instance, Azadi *et al.*[113] evaluated the performance of five different catalysts (*e.g.* Ru/C, Ru/$\gamma$-$Al_2O_3$, Ni/$\gamma$-$Al_2O_3$, Ni/hydrotalcite and RANEY®-Ni catalyst) during the SCWG gasification of glucose, cellulose, fructose, xylan, pulp, lignin and bark. Their results showed that Ni/hydrotalcite and Ni/$\gamma$-$Al_2O_3$ exhibited the best catalytic activity and high $H_2$ selectivity compared to other catalysts tested in the study. They suggested that the behavior of the catalyst was because of their low nickel dispersions and Ni-defect sites compared to other catalysts.

Kang *et al.*[81] tested five different supports (*e.g.* $Al_2O_3$, activated carbon or AC, $TiO_2$, $ZrO_2$ and MgO) and three promoters (*e.g.* Co, Cu and Ce) for Ni-based catalyst. The synthesized catalysts were screened for their performance in the SCWG of lignin. They found that catalytic activity of Ni varied in the order of its support materials as $Al_2O_3$ > $TiO_2$ > AC > $ZrO_2$ > MgO. Likewise, the catalytic activity of Ni-based catalysts for SCWG of lignin using different promoters was in the order of Ce > Co > Cu. The authors reported that Ce improved $H_2$ yield because of its ability to promote Ni dispersion, thereby debilitating the Ni–$Al_2O_3$ interaction.

Lu *et al.*[118] showed that the catalyst support influence both the $H_2$ selectivity, $H_2$ yield and the lifespan of the catalyst. Their experiment involved Ni-based catalyst with different supports.

 

This was done by impregnating $Al_2O_3$ with varying metal oxides (*e.g.* $CeO_2/Al_2O_3$, $La_2O_3/Al_2O_3$, $MgO/Al_2O_3$ and $ZrO_2/Al_2O_3$) and then comparing the performance of each catalyst during the SCWG of glucose. They found the $H_2$ yields for different supports to decrease in the order of $CeO_2/Al_2O_3 > La_2O_3/Al_2O_3 > MgO/Al_2O_3 > Al_2O_3 > ZrO_2/Al_2O_3$. Likewise, the $H_2$ selectivity decreased in the order of $CeO_2/Al_2O_3 > La_2O_3/Al_2O_3 > ZrO_2/Al_2O_3 > Al_2O_3 > MgO/Al_2O_3$. They found that the $H_2$ yield and selectivity reduced because of coke deposition for different catalysts, which ranged between 0.86 and 2.55 g $g^{-1}$ of catalyst. $CeO_2/Al_2O_3$ exhibited the best catalytic activity towards $H_2$ yield (1.35 mol $kg^{-1}$ or ~6 times of the yield obtained without a catalyst) and $H_2$ selectivity (12.35% or ~4 times of the selectivity obtained without a catalyst). This is because of the ability of $CeO_2$ to oxidize the surface-deposited char due to its oxygen mobility and oxygen retaining ability.[118]

In a study by Gong *et al.*,[80] subcritical and supercritical water gasification of humic acid was conducted as a model compound of sewage sludge. The optimal conditions for high $H_2$ yield (0.79 mol $kg^{-1}$) in non-catalytic experiments were 600 °C, 15 wt% humic acid and 75 min. In a sequel study by the same group of researchers, different Lewis acid catalysts at a loading of 15 wt% were found to dramatically enhance the $H_2$ yields (2.79–11.03 mol $kg^{-1}$), total gas yields (4.72–15.44 mol $kg^{-1}$) and $H_2$ gasification efficiency (40.9–141.6%).[79] The activity of Lewis acids in $H_2$ production from sewage sludge model compound (*i.e.* humic acid) was in the order of $AlCl_3 > NiCl_2 > CuCl_2 > FeCl_3 > ZnCl_2 > CaCl_2$. Lewis acids catalyzed the gasification of humic acid and increased $H_2$ yield through ring-opening reactions. In addition, Lewis acids also catalyzed the hydrothermal liquefaction of humic acid to many aromatic and aliphatic components.

Tushar *et al.*[119] studied the use of dual metals (Ni and Ru) and dual supports ($Al_2O_3$ and $ZrO_2$) to improve the $H_2$ yield from SCWG of biocrude obtained from hydrothermal liquefaction of cattle manure at 500–700 °C, 10–20 g $L^{-1}$ carbon concentration and 25 MPa. Glucose was also gasified as a model compound to test the catalytic activity of different synthesized novel catalysts. The synthesized 10% Ni–0.08% $Ru/Al_2O_3$–$ZrO_2$ catalyst revealed the highest $H_2$ yield (1.01 mol $mol^{-1}$ of biocrude and 1.34 mol $mol^{-1}$ of glucose) and maximum carbon gasification efficiency (92% for biocrude and 88% for glucose). The dual catalyst 10% Ni–0.08% $Ru/Al_2O_3$–$ZrO_2$ was found to be highly stable for up to 20 h. Moreover, a study by Kang *et al.*[82] also showed that the catalytic activity and $H_2$ selectivity are dependent on factors such as the method of catalyst support preparation/composition and method of loading the active metals *i.e.* Ni and Co. Co-precipitation method of preparation is found to be superior than the impregnation method.

A recent study by Duan *et al.*[120] showed that a two-component catalyst mixture (Ru/C–Rh/C) employed in the SCWG of microalga *Chlorella pyrenoidosa* exhibited greater catalytic activity compared to a single-component catalyst. They investigated SCWG of *Chlorella* using an equal mixture of Ru/C and Rh/C catalysts. Interestingly, they stated that an increase in SCWG temperature weakens the influence of the catalyst mixture on carbon gasification efficiency and $H_2$ selectivity.

Carbon materials derived from natural sources such as coal and plants residues can be treated through carbonization and activation under high-temperature inert gas, $CO_2$ and/or steam to modify their properties for use as a catalyst or catalyst support for hydrothermal gasification. The physical and chemical properties of treated carbon are dependent on the treatment method and the precursor biomass. Activated carbon is an activated form of char produced from pyrolysis or carbonization followed by chemical or physical activation. Activated carbon (AC) usually has a high surface area (~1500 $m^2$), which is nearly 50 times greater than that of the char.[121] The highly microporous morphology of activated carbons makes them suitable for use as a catalyst or catalyst support.[122,123] Xu *et al.*[124] studied the effects of four different carbon catalysts (*e.g.* spruce wood charcoal, macadamia shell charcoal, coal AC and coconut shell AC) on the gasification of glucose, glycerol, cellobiose, sewage sludge and other biomass waste. The use of 0.6 g of coconut shell activated carbon catalyst decreased the amount of CO produced from 3.18 to 0.79 mol $mol^{-1}$ of feed and increased the carbon gasification efficiency from 80 to 103%. In contrast $H_2$ yield rose from 0.56 to 2.24 mol $mol^{-1}$ of feed with the use of carbon catalyst. However, catalyst deactivation occurred after 4 h of reaction time.

Carbon nanotubes (CNT) have also been viewed as a promising catalytic support for SCWG. CNT are known for their high heat conductivity, open structure, large surface area and most notably their physical and chemical stability.[125] Taylor *et al.*[126] explored the use of Ni catalyst supported by CNT for the SCWG of cellulose in a batch reactor. The synthesized Ni/CNT catalyst produced approximately the same $H_2$ yield (~8 mmol $g^{-1}$) compared to two commercial alumino-silicates supported Ni catalysts. A study by de Vlieger *et al.*[125] revealed the highly stable behavior of Pt/CNT in SCW.

The recovery and reuse of heterogeneous catalyst during SCWG is a significant issue that requires further attention. Catalyst recovery and reuse is important from both environmental and economic perspectives. Catalyst deactivation during SCWG can also occur mainly due to the deposition of carbon materials in form of fine char, thereby blocking the active sites of the catalyst. Therefore, even after recovery of the catalyst during SCWG, effective regeneration is required to restore the catalyst activity.

Furusawa *et al.*[127] investigated the SCWG of lignin in the presence of Ni/MgO catalyst at 400 °C for 120 min with a water density of 0.3 g $cm^{-3}$. They recovered and reused the same catalyst three times and compared the results with and without regeneration treatments. To recover the catalyst, the reaction products were separated into water-insoluble and water-soluble fractions. Furthermore, the water-insoluble fraction containing the catalyst was extracted with tetrahydrofuran (THF) to remove other organic compounds in the product before separating the THF-insoluble fraction containing the catalyst. The recovered THF-insoluble fraction containing the catalyst was regenerated by oxidizing with 10% $O_2$/He mixture at 750 °C to remove the deposited coke and other THF-insoluble components. Despite catalyst regeneration treatments, the catalyst deactivation was still observed. They also observed that catalyst deactivation was

inherent for the reused catalyst without regeneration. They suggested that this behavior could be due to char-like product formation on the catalyst/support surface during SCWG or due to the formation of $Mg(OH)_2$ phase. It was also concluded that irrespective of regeneration treatments, the deactivation of Ni/MgO catalyst is inevitable.

Hossain *et al.*[128] performed catalyst deactivation and regeneration studies on AC catalyst during the hydrothermal gasification of oleic acid. The deactivation of AC catalyst during SCWG was attributed to the deposition of impurities that precedes the decarboxylation reaction and participation in steam reforming reaction during decarboxylation.[128,129] The spent AC catalyst was regenerated by thermal treatment with KOH. The procedure involved mixing the catalyst with KOH followed by heating at 750 °C and 0.5 °C $min^{-1}$ for 3 h under inert atmosphere. KOH was further neutralized with a diluted solution of $HNO_3$ and washing with water to remove the remaining KOH before drying for 12 h. The regenerated and fresh AC catalyst were found to exhibit similar surface properties and product selectivity.[128] It was proposed that thermal treatments with KOH is a low-cost and effective approach for regeneration of carbonaceous catalysts.

## 6. Thermodynamics of hydrothermal gasification

Thermodynamic analysis of $H_2$ production from SCWG of waste biomass and model compounds has been reported by several researchers.[130–133] Thermodynamic analysis helps to develop models that could be useful in the prediction of $H_2$ and total gas yields and composition. This is imperative for reactor designing, process optimization, unit operations, energy recovery studies, techno-economic analysis and lifecycle assessment. Two main thermodynamic approaches are inherent in SCWG research, namely the stoichiometric and non-stoichiometric types.[131] The stoichiometric approach is based on the thermodynamics equilibrium assumption where a certain number of independent reactions consisting of different species are defined. It is easier to identify the respective contribution of each reaction, although it is required to know all the reactions involved in the biomass conversion. On the other hand, the non-stoichiometric approach does not require the reactions to be identified and defined as the equilibrium composition is obtained using the Gibbs free energy minimization method. The procedure involves a prior identification of the species expected in the product, after which calculations are performed to obtain the product distribution that would enable the reaction to approach a minimum Gibbs free energy value. This approach has the advantages of flexibility and ensures that the important reactions are not neglected.[131]

Letellier *et al.*[133] performed the system modeling of a SCWG reactor and a separator for the gasification of aqueous biomass using the stoichiometric approach. Two mathematical models were developed and utilized in their study. The first model was based on the chemical equilibrium assumption used to predict the product leaving the SCWG reactor. The other model was used to predict the separation and expansion steps occurring at the reactor outlet. This latter model assumed physical equilibrium between the gas and liquid phases leaving the system. The model was suitable for the prediction of the process behavior. In another study by Marias *et al.*,[134] SCWG of vinasse (an aqueous residue produced from the alcohol industry) was reported. They developed a model that allowed the simultaneous prediction of solid, liquid and gaseous phases produced during SCWG process together with the energy requirements. They concluded that a mode of operation without the energy requirement can be obtained in an autothermal operational regime *i.e.* feeding an oxidizing agent into the reactor.

Tang and Kitagawa[132] have applied a non-stoichiometric approach to develop a thermodynamic model based on the minimization of Gibbs free energy using the Peng–Robinson equation of state. The model was used to estimate the equilibrium composition during the SCWG of biomass model compounds and real biomass compounds, as well as to study the effect of temperature, pressure and feedstock concentration on $H_2$ yield. Correlating with experimental observations, their findings showed that $H_2$ yield is favored by high temperature, low pressure and feedstock concentration. Castello and Fiori[131] have developed a two-phase non-stoichiometric thermodynamic model to address the challenges relating to the formation of solid carbon during SCWG with the possibility of $NO_x$ formation in certain cases. They concluded that solid char formation is possible when the selected biomass contains high carbon content or at low reaction temperature such as in the case of subcritical water gasification.

Guan *et al.*[135] reported on the SCWG of alga *Nannochloropsis* sp. with 4.7 wt% feed loading at 450–550 °C and water density of 0.087 g $cm^{-3}$. They compared the experimental results with that of thermodynamic modeling using ASPEN Plus software. Their experimental results showed proximity to the thermodynamic equilibrium values. The carbon yield and energy recovery amplified at higher temperature, longer reaction time and greater water density. The formation of gas products such as $H_2$, $CO_2$ and $CH_4$ followed individual reaction pathways, which was evident from their different activation energies. Besides, it was also reported that the char yield, gas composition and energy recovery during SCWG of biomass are system specific and largely depend on the process variables.

## 7. Conclusions

SCWG is a promising technology to convert lignocellulosic biomass with high moisture content into sustainable fuels. With the advent of climate change, energy shortages and environmental issues, SCWG can be a feasible option to supply $H_2$ that can replace fossil fuels. SCWG of lignocellulosic biomass was the focus of this review. We attempt to bridge the gap between the past research progress and the future perspectives. Regarding the commercialization of SCWG several economic issues and knowledge gaps identified are outlined below:

(i) Most of the studies carried out on SCWG involved the use of biomass model compounds. However, more research on real biomass is required to understand their decomposition

 

behavior in aqueous environment and foresee the challenges in large scale operations. Such studies could provide detailed understanding of the issues of real biomass complexity.

(ii) In low-temperature catalytic SCWG, there has been enormous progress in the use of homogeneous catalysts, especially alkali carbonates to improve gas yields. However, the recyclability of homogeneous catalyst is still an issue that needs further attention.

(iii) Integration of SCWG process with Fischer–Tropsch synthesis as a potential biomass–gas–liquid conversion technology could be a win–win scenario in terms of environmental perspective and the commercial market. Although promising, practical implementation of such an approach is rare in literature. Since SCWG-derived syngas contains less impurities compared to coal gasification-derived syngas, this could significantly reduce the syngas cleanup cost prior to Fischer–Tropsch synthesis.

(iv) High-temperature and high-pressure requirement of SCWG means that there are many concerns associated with the process such as material corrosion and durability as well as waste heat generation. Recovery of waste heat during SCWG and its reuse within the processing plant or for power generation can considerably supplement the all-inclusive process expenditures relating to energy input. In conclusion, SCWG has immense potential towards the conversion of waste biomass to produce biofuels. Further research and development related to SCWG should continue to overcome the limitations associated with the technology.

## Conflicts of interest

There are no conflicts to declare.

## Acknowledgements

The financial support from Natural Sciences and Engineering Research Council (NSERC) of Canada and Canada Research Chair (CRC) program is greatly acknowledged.

## References

1 S. Nanda, R. Azargohar, A. K. Dalai and J. A. Kozinski, *Renewable Sustainable Energy Rev.*, 2015, **50**, 925–941.
2 S. Nanda, J. A. Kozinski and A. K. Dalai, *Curr. Biochem. Eng.*, 2016, **3**, 24–36.
3 S. Nanda, A. K. Dalai and J. A. Kozinski, *Energy Sci. Eng.*, 2014, **2**, 138–148.
4 R. Ren, X. Han, H. Zhang, H. Lin, J. Zhao, Y. Zheng and H. Wang, *Carbon Resources Conversion*, 2018, **1**, 153–159.
5 J. S. Tumuluru, C. T. Wright, J. R. Hess and K. L. Kenney, *Biofuels, Bioprod. Biorefin.*, 2011, **5**, 683–707.
6 Y. Qian, C. Zuo, J. Tan and J. He, *Energy*, 2007, **32**, 196–202.
7 S. Nanda, P. Mohanty, K. K. Pant, S. Naik, J. A. Kozinski and A. K. Dalai, *BioEnergy Res.*, 2013, **6**, 663–677.
8 S. N. Reddy, S. Nanda, U. G. Hegde, M. C. Hicks and J. A. Kozinski, *RSC Adv.*, 2015, **5**, 36404–36422.
9 A. Kruse, *Biofuels, Bioprod. Biorefin.*, 2008, **2**, 415–437.
10 P. Basu and V. Mettanant, *Int. J. Chem. React. Eng.*, 2009, **7**, DOI: 10.2202/1542-6580.1919.
11 P. Kritzer, *J. Supercrit. Fluids*, 2004, **29**, 1–29.
12 W. Feng, H. J. van der Kooi and J. S. Arons, *Chem. Eng. Process.*, 2004, **43**, 1459–1467.
13 P. T. Williams and J. Onwudili, *Energy Fuels*, 2006, **20**, 1259–1265.
14 A. A. Peterson, F. Vogel, R. P. Lachance, M. Fröling, M. J. Antal Jr and J. W. Tester, *Energy Environ. Sci.*, 2008, **1**, 32–65.
15 Y. Guo, S. Z. Wang, D. H. Xu, Y. M. Gong, H. H. Ma and X. Y. Tang, *Renewable Sustainable Energy Rev.*, 2010, **14**, 334–343.
16 S. N. Reddy, N. Ding, S. Nanda, A. K. Dalai and J. A. Kozinski, *Biofuels, Bioprod. Biorefin.*, 2014, **8**, 728–737.
17 S. N. Reddy, S. Nanda, A. K. Dalai and J. A. Kozinski, *Int. J. Hydrogen Energy*, 2014, **39**, 6912–6926.
18 C. R. Correa and A. Kruse, *J. Supercrit. Fluids*, 2017, **133**, 573–590.
19 A. T. W. M. Hendriks and G. Zeeman, *Bioresour. Technol.*, 2009, **100**, 10–18.
20 S. Nanda, J. Maley, J. A. Kozinski and A. K. Dalai, *J. Biobased Mater. Bioenergy*, 2015, **9**, 295–308.
21 F. L. P. Resende, M. E. Neff and P. E. Savage, *Energy Fuels*, 2007, **21**, 3637–3643.
22 X. Hao, L. Guo, X. Zhang and Y. Guan, *Chem. Eng. J.*, 2005, **1–3**, 57–65.
23 T. Yoshida and Y. Matsumura, *Ind. Eng. Chem. Res.*, 2001, **40**, 5469–5474.
24 C. Cao, L. Guo, Y. Chen, S. Guo and Y. Lu, *Int. J. Hydrogen Energy*, 2011, **36**, 13528–13535.
25 N. Ding, R. Azargohar, A. K. Dalai and J. A. Kozinski, *Fuel*, 2014, **118**, 416–425.
26 A. Demirbas, *Int. J. Hydrogen Energy*, 2004, **29**, 1237–1243.
27 S. Nanda, J. Isen, A. K. Dalai and J. A. Kozinski, *Energy Convers. Manage.*, 2016, **110**, 296–306.
28 I. G. Lee, M. S. Kim and S. K. Ihm, *Ind. Eng. Chem. Res.*, 2002, **41**, 1182–1188.
29 K. Kang, R. Azargohar, A. K. Dalai and H. Wang, *Energy Fuels*, 2015, **29**, 1776–1784.
30 J. Louw, C. E. Schwarz and A. J. Burger, *Bioresour. Technol.*, 2016, **201**, 111–120.
31 S. Nanda, M. Gong, H. N. Hunter, A. K. Dalai, I. Gökalp and J. A. Kozinski, *Fuel Process. Technol.*, 2017, **168**, 84–96.
32 T. Yoshida, Y. Oshima and Y. Matsumura, *Biomass Bioenergy*, 2004, **26**, 71–78.
33 S. Nanda, A. K. Dalai and J. A. Kozinski, *Biomass Bioenergy*, 2016, **95**, 378–387.
34 M. J. Antal Jr, Y. Matsumura, X. Xu, J. Stenberg and P. Lipnik. *Preprints of Papers*, American Chemical Society, Division of Fuel Chemistry, 1995, pp. 304–307.
35 M. H. Waldner and F. Vogel, *Ind. Eng. Chem. Res.*, 2005, **44**, 4543–4551.
36 D. S. Gokkaya, M. Saglam, M. Yuksel and L. Ballice, *Biomass Bioenergy*, 2016, **91**, 26–36.
37 Y. J. Lu, L. J. Guo, C. M. Ji, X. M. Zhang, X. H. Hao and Q. H. Yan, *Int. J. Hydrogen Energy*, 2006, **31**, 822–831.

38 S. Nanda, J. Mohammad, S. N. Reddy, J. A. Kozinski and A. K. Dalai, *Biomass Convers. Biorefin.*, 2014, **4**, 157–191.
39 T. Istirokhatun, N. Rokhati, R. Rachmawaty, M. Meriyani, S. Priyanto and H. Susanto, *Procedia Environ. Sci.*, 2015, **23**, 274–281.
40 S. Prasad, A. Singh and H. C. Joshi, *Resour., Conserv. Recycl.*, 2007, **50**, 1–39.
41 J. Yanik, S. Ebale, A. Kruse, M. Saglam and M. Yüksel, *Fuel*, 2007, **86**, 2410–2415.
42 M. Ayyachamy, F. E. Cliffe, J. M. Coyne, J. Collier and M. G. Tuohy, *Biomass Convers. Biorefin.*, 2013, **3**, 255–269.
43 M. Osada, T. Sato, M. Watanabe, T. Adschiri and K. Arai, *Energy Fuels*, 2004, **18**, 327–333.
44 U. Hasanah, B. Setiaji and C. Anwar, *J. Pure Appl. Chem. Res.*, 2012, **1**, 26–32.
45 S. Nanda, S. N. Reddy, A. K. Dalai and J. A. Kozinski, *Int. J. Hydrogen Energy*, 2016, **41**, 4907–4921.
46 Z. Fang, T. Sato, R. L. Smith Jr, H. Inomata, K. Arai and J. A. Kozinski, *Bioresour. Technol.*, 2008, **99**, 3424–3430.
47 M. Carrier, A. Loppinet-Serani, D. Denux, J. M. Lasnier, F. Ham-Pichavant, F. Cansell and C. Aymonier, *Biomass Bioenergy*, 2011, **35**, 298–307.
48 T. Furusawa, T. Sato, H. Sugito, Y. Miura, Y. Ishiyama, M. Sato, N. Itoh and N. Suzuk, *Int. J. Hydrogen Energy*, 2007, **32**, 699–704.
49 M. Shirai, Y. Murakami, N. Hiyoshi, N. Mimura, A. Yamaguchi and O. Sato, *J. Mol. Catal. A: Chem.*, 2014, **388–389**, 148–153.
50 S. Nanda, R. Rana, Y. Zheng, J. A. Kozinski and A. K. Dalai, *Sustainable Energy Fuels*, 2017, **1**, 1232–1245.
51 L. J. Guo, Y. J. Lu, X. M. Zhang, C. M. Ji, Y. Guan and A. X. Pei, *Catal. Today*, 2007, **129**, 275–286.
52 R. F. Susanti, B. Veriansyah, J. D. Kim, J. Kim and Y. W. Lee, *Int. J. Hydrogen Energy*, 2010, **35**, 1957–1970.
53 S. Nanda, S. N. Reddy, H. N. Hunter, A. K. Dalai and J. A. Kozinski, *J. Supercrit. Fluids*, 2015, **104**, 112–121.
54 B. M. Kabyemela, T. Adschiri, R. M. Malaluan and K. Arai, *Ind. Eng. Chem. Res.*, 1999, **38**, 2888–2895.
55 D. Castello, A. Kruse and L. Fiori, *Biomass Bioenergy*, 2015, **73**, 84–94.
56 M. Saisu, T. Sato, M. Watanabe, T. Adschiri and K. Arai, *Energy Fuels*, 2003, **17**, 922–928.
57 Z. Fang, T. Minowa, C. Fang, R. L. Smith, H. Inomata and J. A. Kozinski, *Int. J. Hydrogen Energy*, 2008, **33**, 981–990.
58 A. Kruse, P. Bernolle, N. Dahmen, E. Dinjus and P. Maniam, *Energy Environ. Sci.*, 2010, **3**, 136–143.
59 Y. Su, W. Zhu, M. Gong, H. Zhou, Y. Fan and B. Amuzu-Sefordzi, *Int. J. Hydrogen Energy*, 2015, **40**, 9125–9136.
60 K. Okuda, M. Umetsu, S. Takami and T. Adschiri, *Fuel Process. Technol.*, 2004, **85**, 803–813.
61 P. E. Savage, *J. Supercrit. Fluids*, 2009, **47**, 407–414.
62 A. Chuntanapum and Y. Matsumura, *Ind. Eng. Chem. Res.*, 2010, **49**, 4055–4062.
63 S. N. Reddy, S. Nanda and J. A. Kozinski, *Chem. Eng. Res. Des.*, 2016, **113**, 17–27.
64 C. Promdej and Y. Matsumura, *Ind. Eng. Chem. Res.*, 2011, **50**, 8492–8497.
65 P. D'Jesús, N. Boukis, B. Kraushaar-Czarnetzki and E. Dinjus, *Fuel*, 2006, **85**, 1032–1038.
66 R. Rana, S. Nanda, J. A. Kozinski and A. K. Dalai, *J. Environ. Chem. Eng.*, 2018, **6**, 182–189.
67 S. Nanda, R. Rana, H. N. Hunter, Z. Fang, A. K. Dalai and J. A. Kozinski, *Chem. Eng. Sci.*, 2018, DOI: 10.1016/j.ces.2018.10.039.
68 T. Yoshida and Y. Matsumura, *Ind. Eng. Chem. Res.*, 2009, **48**, 8381–8386.
69 V. Anikeev and M. Fan, *Supercritical Fluid Technology for Energy and Environmental Applications*, Elsevier, Amsterdam, The Netherlands, 2013.
70 W. Bühler, E. Dinjus, H. J. Ederer, A. Kruse and C. Mas, *J. Supercrit. Fluids*, 2002, **22**, 37–53.
71 J. B. Gadhe and R. B. Gupta, *Ind. Eng. Chem. Res.*, 2005, **44**, 4577–4585.
72 A. J. Byrd, K. K. Pant and R. B. Gupta, *Energy Fuels*, 2007, **21**, 3541–3547.
73 D. Yu, M. Aihara and M. J. Antal, *Energy Fuels*, 1993, **7**, 574–577.
74 G. Chen, J. Andries, Z. Luo and H. Spliethoff, *Energy Convers. Manage.*, 2003, **44**, 1875–1884.
75 S. Guo, L. Guo, C. Cao, J. Yin, Y. Lu and X. Zhang, *Int. J. Hydrogen Energy*, 2012, **37**, 5559–5568.
76 P. T. Williams and J. Onwudili, *Ind. Eng. Chem. Res.*, 2005, **44**, 8739–8749.
77 P. Azadi and R. Farnood, *Int. J. Hydrogen Energy*, 2011, **36**, 9529–9541.
78 S. Nanda, A. K. Dalai, I. Gökalp and J. A. Kozinski, *Waste Manage.*, 2016, **52**, 147–158.
79 M. Gong, S. Nanda, H. N. Hunter, W. Zhu, A. K. Dalai and J. A. Kozinski, *Catal. Today*, 2017, **291**, 13–23.
80 M. Gong, S. Nanda, M. J. Romero, W. Zhu and J. A. Kozinski, *J. Supercrit. Fluids*, 2017, **119**, 130–138.
81 K. Kang, R. Azargohar, A. K. Dalai and H. Wang, *Chem. Eng. J.*, 2016, **283**, 1019–1032.
82 K. Kang, R. Azargohar, A. K. Dalai and H. Wang, *Int. J. Energy Res.*, 2017, **41**, 1835–1846.
83 R. L. Smith Jr and Z. Fang, *J. Supercrit. Fluids*, 2009, **47**, 431–446.
84 P. E. Bocanegra, C. Reverte, C. Aymonier, A. Loppinet-Serani, M. M. Barsan, I. S. Butler, J. A. Kozinski and I. Gökalp, *J. Supercrit. Fluids*, 2010, **53**, 72–81.
85 W. A. Bassett, *Eur. J. Mineral.*, 2003, **15**, 773–780.
86 M. Sasaki, Z. Fang, Y. Fukushima, T. Adschiri and K. Arai, *Ind. Eng. Chem. Res.*, 2000, **39**, 2883–2890.
87 S. Nanda, S. N. Reddy, H. N. Hunter, I. S. Butler and J. A. Kozinski, *Ind. Eng. Chem. Res.*, 2015, **54**, 9296–9306.
88 A. Kruse and M. Faquir, *Chem. Eng. Technol.*, 2007, **30**, 749–754.
89 Y. Matsumura and T. Minowa, *Int. J. Hydrogen Energy*, 2004, **29**, 701–707.
90 S. Hirota, S. Inoue, T. Inoue, Y. Kawai, Y. Wada, T. Noguchi and Y. Matsumura, *Korean J. Chem. Eng.*, 2016, **33**, 1261–1266.
91 Y. J. Lu, H. Jin, L. J. Guo, X. M. Zhang, C. Q. Cao and X. Guo, *Int. J. Hydrogen Energy*, 2008, **33**, 6066–6075.

 

92 O. Norouzi, F. Safari, S. Jafarian, A. Tavasoli and A. Karimi, *Energy Convers. Manage.*, 2017, **141**, 63–71.
93 I. Deniz, F. Vardar-Sukan, M. Yüksel, M. Saglam, L. Ballice and O. Yesil-Celiktas, *Energy Convers. Manage.*, 2015, **96**, 124–130.
94 Z. Fang, T. Minowa, R. L. Smith, T. Ogi and J. A. Koziński, *Ind. Eng. Chem. Res.*, 2004, **43**, 2454–2463.
95 B. Veriansyah, J. Kim, J. D. Kim and Y. W. Lee, *Int. J. Green Energy*, 2008, **5**, 322–333.
96 W. Cao, C. Cao, L. Guo, H. Jin, M. Dargusch, D. Bernhardt and X. Yao, *Int. J. Hydrogen Energy*, 2016, **41**, 22722–22731.
97 Y. Chen, L. Guo, W. Cao, H. Jin, S. Guo and X. Zhang, *Int. J. Hydrogen Energy*, 2013, **38**, 12991–12999.
98 N. Boukis, U. Galla, H. Müller and E. Dinjus, *15th European Conference & Exhibition*, Berlin, 2007, pp. 1013–1016.
99 Y. Matsumura, in *Recent Advances in Thermo-Chemical Conversion of Biomass*, ed. A. Pandey, T. Bhaskar, M. Stöcker, and R. Sukumaran, Elsevier, Netherlands, 2015, pp. 251–267.
100 O. Yakaboylu, I. Albrecht, J. Harinck, K. G. Smit, G. A. Tsalidis, M. Di Marcello, K. Anastasakis and W. de Jong, *Biomass Bioenergy*, 2018, **111**, 330–342.
101 S. van Wyk, S. O. Odu, A. G. van der Ham and S. R. Kersten, *Desalination*, 2018, **439**, 80–92.
102 D. Xu, S. Wang, X. Hu, C. Chen, Q. Zhang and Y. Gong, *Int. J. Hydrogen Energy*, 2009, **34**, 5357–5364.
103 J. C. Juan, D. A. Kartika, T. Y. Wu and T. Y. Y. Hin, *Bioresour. Technol.*, 2011, **102**, 452–460.
104 A. Sınağ, A. Kruse and J. Rathert, *Ind. Eng. Chem. Res.*, 2004, **43**, 502–508.
105 A. Kruse, A. Krupka, V. Schwarzkopf, C. Gamard and T. Henningsen, *Ind. Eng. Chem. Res.*, 2005, **44**, 3013–3020.
106 J. A. Onwudili and P. T. Williams, *Int. J. Hydrogen Energy*, 2009, **34**, 5645–5656.
107 T. G. Madenoğlu, N. Boukis, M. Sağlam and M. Yüksel, *Int. J. Hydrogen Energy*, 2011, **36**, 14408–14415.
108 T. G. Madenoğlu, E. Yıldırır, M. Sağlam, M. Yüksel and L. Ballice, *J. Supercrit. Fluids*, 2014, **95**, 339–347.
109 Y. Richardson, J. Blin and A. Julbe, *Prog. Energy Combust. Sci.*, 2012, **38**, 765–781.
110 X. H. Hao, L. J. Guo, M. Mao, X. M. Zhang and X. J. Chen, *Int. J. Hydrogen Energy*, 2003, **28**, 55–64.
111 M. J. Sheikhdavoodi, M. Almassi, M. Ebrahimi-Nik, A. Kruse and H. Bahrami, *J. Energy Inst.*, 2015, **88**, 450–458.
112 F. L. P. Resende and P. E. Savage, *Ind. Eng. Chem. Res.*, 2010, **49**, 2694–2700.
113 P. Azadi, S. Khan, F. Strobel, F. Azadi and R. Farnood, *Appl. Catal., B*, 2012, **117–118**, 330–338.
114 S. Li, L. Guo, C. Zhu and Y. Lu, *Int. J. Hydrogen Energy*, 2013, **38**, 9688–9700.
115 K. Bru, J. Blin, A. Julbe and G. Volle, *J. Anal. Appl. Pyrolysis*, 2007, **78**, 291–300.
116 Y. Richardson, J. Blin, G. Volle, J. Motuzas and A. Julbe, *Appl. Catal., A*, 2010, **382**, 220–230.
117 Y. Richardson, J. Motuzas, A. Julbe, G. Volle and J. Blin, *J. Phys. Chem. C*, 2013, **117**, 23812–23831.
118 Y. Lu, Y. Zhu, S. Li, X. Zhang and L. Guo, *Biomass Bioenergy*, 2014, **67**, 125–136.
119 M. S. H. K. Tushar, A. Dutta and C. C. Xu, *Appl. Catal., B*, 2016, **189**, 119–132.
120 P. G. Duan, S. C. Li, J. L. Jiao, F. Wang and Y. P. Xu, *Sci. Total Environ.*, 2018, **630**, 243–253.
121 S. Nanda, A. K. Dalai, F. Berruti and J. A. Kozinski, *Waste Biomass Valorization*, 2016, **7**, 201–235.
122 R. Rana, S. Nanda, A. Maclennan, Y. Hu, J. A. Kozinski and A. K. Dalai, *J. Energy Chem.*, 2018, DOI: 10.1016/j.jechem.2018.05.012.
123 E. Lam and J. H. T. Luong, *ACS Catal.*, 2014, **4**, 3393–3410.
124 X. Xu, Y. Matsumura, J. Stenberg and M. J. Antal, *Ind. Eng. Chem. Res.*, 1996, **35**, 2522–2530.
125 D. J. M. de Vlieger, D. B. Thakur, L. Lefferts and K. Seshan, *ChemCatChem*, 2012, **4**, 2068–2074.
126 A. D. Taylor, G. J. DiLeo and K. Sun, *Appl. Catal., B*, 2009, **93**, 126–133.
127 T. Furusawa, T. Sato, M. Saito, Y. Ishiyama, M. Sato, N. Itoh and N. Suzuki, *Appl. Catal., A*, 2007, **327**, 300–310.
128 M. Z. Hossain, A. K. Jhawar, M. B. Chowdhury, W. Z. Xu and P. A. Charpentier, *Fuel*, 2018, **231**, 253–263.
129 M. Z. Hossain, A. K. Jhawar, M. B. Chowdhury, W. Z. Xu, W. Wu, D. V. Hiscott and P. A. Charpentier, *Energy Fuels*, 2017, **31**, 4013–4023.
130 O. Yakaboylu, J. Harinck, K. G. Gerton Smit and W. de Jong, *Biomass Bioenergy*, 2013, **59**, 253–263.
131 D. Castello and L. Fiori, *Bioresour. Technol.*, 2011, **102**, 7574–7582.
132 H. Tang and K. Kitagawa, *Chem. Eng. J.*, 2005, **106**, 261–267.
133 S. Letellier, F. Marias, P. Cezac and J. P. Serin, *J. Supercrit. Fluids*, 2010, **51**, 353–361.
134 F. Marias, S. Letellier, P. Cezac and J. P. Serin, *Biomass Bioenergy*, 2011, **35**, 59–73.
135 Q. Guan, P. E. Savage and C. Wei, *J. Supercrit. Fluids*, 2012, **61**, 139–145.